ASTROBIOLOGY
Volume 17, Number 10, 2017
Mary Ann Liebert, Inc.
DOI: 10.1089/ast.2016.1578

Review Article

Reflections on O_2 as a Biosignature in Exoplanetary Atmospheres

Victoria S. Meadows[1,2]

Abstract

Oxygenic photosynthesis is Earth's dominant metabolism, having evolved to harvest the largest expected energy source at the surface of most terrestrial habitable zone planets. Using CO_2 and H_2O—molecules that are expected to be abundant and widespread on habitable terrestrial planets—oxygenic photosynthesis is plausible as a significant planetary process with a global impact. Photosynthetic O_2 has long been considered particularly robust as a sign of life on a habitable exoplanet, due to the lack of known ''false positives''—geological or photochemical processes that could also produce large quantities of stable O_2. O_2 has other advantages as a biosignature, including its high abundance and uniform distribution throughout the atmospheric column and its distinct, strong absorption in the visible and near-infrared. However, recent modeling work has shown that false positives for abundant oxygen or ozone could be produced by abiotic mechanisms, including photochemistry and atmospheric escape. Environmental factors for abiotic O_2 have been identified and will improve our ability to choose optimal targets and measurements to guard against false positives. Most of these false-positive mechanisms are dependent on properties of the host star and are often strongest for planets orbiting M dwarfs. In particular, selecting planets found within the conservative habitable zone and those orbiting host stars more massive than 0.4 $M_\odot$ (M3V and earlier) may help avoid planets with abundant abiotic O_2 generated by water loss. Searching for O_4 or CO in the planetary spectrum, or the lack of H_2O or CH_4, could help discriminate between abiotic and biological sources of O_2 or O_3. In advance of the next generation of telescopes, thorough evaluation of potential biosignatures—including likely environmental context and factors that could produce false positives—ultimately works to increase our confidence in life detection. Key Words: Biosignatures—Exoplanets—Oxygen—Photosynthesis—Planetary spectra. Astrobiology 17, 1022–1052.

1. Introduction

Powered by our parent star, oxygenic photosynthesis is the dominant metabolism on our planet and is arguably the easiest to detect over interstellar distances. In addition to fueling the organisms that use it, oxygenic photosynthesis also creates a highly useful environmental energy gradient between oxygen and reduced organic carbon, the recombination of which produces sufficient energy to support multicellular, differentiated organisms (*e.g.,* Hedges *et al.,* 2004; Catling *et al.,* 2005; Falkowski and Godfrey, 2008; Reinhard *et al.,* 2016). Photosynthetic organisms, including cyanobacteria and vegetation, have left a global mark on Earth's current environment—significantly modifying its atmosphere, surface, geochemical cycling, ecological structure, and seasonal appearance (Meadows, 2008; Meadows and Seager, 2010). The strongest and most widely recognized sign of life on our planet is photosynthetically generated O_2, which is evenly mixed throughout the atmospheric column and composes 21% of our atmosphere. O_2 is also spectrally active at visible and near-IR (NIR) wavelengths; consequently, abundant oxygen will likely be the first sign of life that we search for on extrasolar planets with next-generation telescopes (Des Marais *et al.,* 2002; Brandt and Spiegel, 2014; Misra *et al.,* 2014a).

Phototrophs can also produce surface reflectance and seasonally dependent biosignatures, which could be sought as a secondary confirmation of a biospheric source for abundant O_2. The vegetation red edge is currently Earth's dominant surface biosignature, producing a sharp rise in reflectivity longward of chlorophyll absorption at 688 nm (Gates *et al.,*

[1]Department of Astronomy and Astrobiology Program, University of Washington, Seattle, Washington.
[2]NASA Astrobiology Institute—Virtual Planetary Laboratory, USA.

1965). This effect produces a 2% variation in Earth's disk-averaged spectrum, as vegetated hemispheres of Earth replace ocean-dominated views (Arnold *et al.,* 2002; Montañés-Rodríguez *et al.,* 2006; Tinetti *et al.,* 2006b; Arnold, 2008). Many photosynthetic microorganisms, including algae and bacterial mats, produce similar characteristic reflectivity rises but at different wavelengths (Kiang *et al.,* 2007a; Hegde *et al.,* 2015). Time-dependent signs of photosynthetic life include the seasonal cycles of surface vegetation coverage and the annual cycle of global atmospheric CO_2 abundance. The latter occurs as phototrophs draw down CO_2 in the spring and summer during their productive growth phase and release it back to the atmosphere when vegetation dies and decays in autumn and winter. This cycle produces a 1–2% change in the CO_2 abundance over the year (Keeling *et al.,* 1976, 1996; Bacastow *et al.,* 1985), and its amplitude in the global average is a function of our land mass distribution and obliquity.

Although it requires complicated molecular machinery (Blankenship, 2010; Hohmann-Marriott and Blankenship, 2012), some form of photosynthesis is highly plausible as an eventually significant life process on extrasolar habitable planets. In particular, the environmental resources required to fuel and drive photosynthesis are likely common on a terrestrial planet in the surface liquid water habitable zone—that region around a star in which an Earth-like planet could support liquid water on its surface (Kasting *et al.,* 1993; Kopparapu *et al.,* 2013). Oxygenic photosynthesis uses light from the parent star—the ubiquitous and likely dominant energy source for a planet in the habitable zone; carbon dioxide—a common molecule in Solar System terrestrial planet atmospheres; and liquid water—which is expected to be abundant on a classically defined habitable planet. By using these globally available and energetically rich components of the habitable terrestrial environment, oxygenic photosynthesis would have a significant evolutionary advantage, allowing it to dominate its planetary surface environment (Kiang *et al.,* 2007b; Léger *et al.,* 2011; Kiang, 2014), which in turn would make it more detectable on a planetary scale. On our own planet, oxygenic phototrophs have been able to colonize a significant fraction of Earth's surface, populating marine, freshwater, and terrestrial habitats, including extreme environments such as hot springs (Ward and Castenholz, 2000), hypersaline settings (Oren, 2015), and polar regions (Painter *et al.,* 2001; Vincent, 2002; Williams *et al.,* 2003).

Earth's photosynthesis is also an ancient metabolic process that, despite its apparent complexity, developed relatively rapidly—appearing within a billion years after the Moon-forming impact. Multiple geological and geochemical lines of evidence suggest that anoxygenic photosynthesizers were present on Earth by at least 3.3 Ga (Westall *et al.,* 2011) and possibly as far back as 3.5 Ga (Buick *et al.,* 1981) or 3.7 Ga (Nutman *et al.,* 2016). These early anoxygenic phototrophs likely used strong reductants such as hydrogen or hydrogen sulfide—rather than the water used by oxygenic phototrophs—to donate electrons to a single photosystem that harvested light (Olson and Pierson, 1986). These reductants were produced by geological processes such as volcanism and would have been present in sufficient concentration to drive photosynthesis in only a relatively limited number of environments. Consequently, anoxygenic photosynthesizers would have been challenging to detect remotely in the global average, as they were spatially restricted to these sources of strong reductants and are not known to produce gaseous by-products. The best way to detect these anoxygenic phototrophic organisms remotely may have been via their surface reflectivity signal (*e.g.,* Sanromá *et al.,* 2013, 2014). Nonphotosynthetic pigments developed for other purposes by phototrophs—including environmental survival (Dartnell, 2011)—may also produce surface reflectivity biosignatures prior to the rise of oxygen—both for the early Earth and on other planets (Schwieterman *et al.,* 2015a).

The limited environments suitable for early anoxygenic photosynthesizers provided evolutionary pressure for the development of a second photosystem that, when linked to the other, could use weaker—but abundant and globally widespread—reductants such as water, and produce oxygen as a waste product (Blankenship, 2010). The timing of the origin of oxygenic photosynthesis is not known but can be constrained by its subsequent impact on the environment. Geological evidence for oxidative weathering of continents suggests that O_2 may have temporarily risen to appreciable levels in our atmosphere as far back as 2.5 Ga (Anbar *et al.,* 2007; Kaufman *et al.,* 2007; Buick, 2008; Lyons *et al.,* 2014). This evidence for early O_2 production was subsequently confirmed by nitrogen (Garvin *et al.,* 2009) and selenium (Stüeken *et al.,* 2015a) isotope studies. Biomarkers in fluid inclusions also suggest that oxygenic photosynthesis was active at 2.45 Ga (Dutkiewicz *et al.,* 2006; George *et al.,* 2008, 2009). However, more recent isotope measurements point to transient low levels of O_2 that may have existed at even earlier times, potentially pushing the environmental impact of oxygenic photosynthesis back to 3.0–2.65 Ga (Czaja *et al.,* 2012; Crowe *et al.,* 2013; Planavsky *et al.,* 2014a; Riding *et al.,* 2014). Yet the irreversible, global accumulation of O_2 in the atmosphere—likely mediated by burial and removal of organic carbon from Earth's surface environment (Kasting, 2001; Lyons *et al.,* 2014)—evidently occurred somewhat later, between 2.45 and 2.2 Ga (Farquhar *et al.,* 2000; Bekker *et al.,* 2004; Canfield, 2005), with recent sulfur isotope studies (Luo *et al.,* 2016) placing it at 2.33 Ga. Recent evidence suggests that the rise of oxygen to its modern high levels in Earth's atmosphere may have been delayed even further, to 0.8 Ga (Planavsky *et al.,* 2014b), long after the advent of oxygenic photosynthesis.

2. O_2 as a Biosignature

For an atmospheric gas to audition for the role of planetary biosignature, it must be produced predominantly by life, build up to detectable levels in the atmosphere by resisting destruction or sequestration in the planetary environment, and exhibit strong spectral signatures that are within the wavelength range of planned astronomical instrumentation (*e.g.,* Domagal-Goldman *et al.,* 2011; Seager *et al.,* 2012). Photosynthetic O_2 excels in meeting all three criteria. It is the volatile by-product of the metabolism driven by the dominant source of energy on our planet's surface. Over time O_2 has risen to be the second most abundant gas in our atmosphere, after the dominant N_2—which may also be biologically mediated through biological fixation, mineral absorption, and sequestration into the mantle (Catling and Kasting, 2007; Johnson and Goldblatt, 2015). The less abundant O_2, however, still wins in spectral detectability. N_2 is a homonuclear molecule with no permanent

dipole, and it absorbs strongly only in the ultraviolet (80–100 nm)—a region that is crowded with UV bands from many species that may be common in terrestrial planet atmospheres, including H_2O, CO_2, CO, O_2, CH_4, and other hydrocarbons (Rothman *et al.,* 2013). The spectral region below 100 nm is also not accessible by ground-based telescopes due to strong absorption by N_2 in Earth's atmosphere. It is also challenging to observe from space, primarily due to sharp decreases in mirror reflectivity, even for UV-optimized mirror coatings (*e.g.,* Hennessy *et al.,* 2016). Reflected light observations of the planet in this wavelength region are also hampered by the relatively low UV flux from the star, and therefore from the planet, when compared to visible light observations.

In comparison, abundant atmospheric oxygen produces several strong and distinct features throughout the UV to mid-IR (MIR) from either O_2 itself, from its photochemical by-product, O_3, or from collisional production of O_4 molecules (Richard *et al.,* 2012). O_2 has strong features at UV wavelengths <0.2 μm and in the visible/NIR. The latter include the γ band at 0.628 μm, B-band at 0.688 μm, A-band at 0.762 μm, and the $a\ ^1\Delta_g$ band at 1.269 μm; the A-band is the strongest of these (Rothman *et al.,* 2013). O_2 collisional pairs (O_4) form preferentially in high-density, high-O_2 atmospheres, although O_4 can also be seen in Earth's disk-averaged and transmission spectra (Tinetti *et al.,* 2006a; Pallé *et al.,* 2009). O_4 exhibits several features from 0.3–0.7 μm (Hermans *et al.,* 1999; Thalman and Volkamer, 2013), as well as at 1.06 (Greenblatt *et al.,* 1990) and 1.269 μm (Maté *et al.,* 1999; Misra *et al.,* 2014a; Schwieterman *et al.,* 2016a, 2016b). This latter O_4 band coincides with the O_2 $a\ ^1\Delta_g$ band and O_2-N_2 collisionally induced absorption (Smith and Newnham, 2000; Pallé *et al.,* 2009), which can complicate its detailed interpretation, although all these features clearly indicate the presence of O_2. The presence of O_2 may also be inferred from its photochemical by-product, O_3 (Ratner and Walker, 1972), which has strong bands in the UV (0.2–0.3 μm), visible (0.5–0.7 μm) and MIR (9.6 μm) (Rothman *et al.,* 2013). In the MIR, O_3 is considered a more detectable proxy for the presence of oxygen (Segura *et al.,* 2003, 2005), as in this wavelength range O_2 has only extremely weak absorption at wavelengths within the strong 6.3 μm water band. However, O_3 can also be produced by the photolysis of other oxygen-bearing compounds, such as CO_2 and H_2O. The superior detectability of O_2 and its photochemical by-products has contributed to O_2 and/or O_3 being a biosignature focus for missions that are being planned to search for evidence of life on exoplanets, including most recently the Exo-Coronography (Stapelfeldt *et al.,* 2015), Exo-Starshade (Seager *et al.,* 2015), and High-Definition Space Telescope concepts (*e.g.,* Dalcanton *et al.,* 2015; Rioux *et al.,* 2015).

In addition to its strong absorption features in the visible and NIR, oxygen has another significant advantage as a biosignature because it is more likely to be evenly mixed throughout the atmospheric column, making it accessible to observation by transit spectroscopy. On Earth our abundant atmospheric O_2 maintains a near-constant mixing ratio throughout the troposphere, stratosphere, and much of the upper atmosphere. This is due to relatively low volcanic outgassing rates, a lack of strong surface sinks from our oxidized crust, and O_2's relative robustness to photolytic destruction in the stratosphere. As transit spectroscopy cannot probe as deeply into an atmosphere as direct imaging due to either the presence of high clouds or hazes (Kreidberg *et al.,* 2014; Charnay *et al.,* 2015; Arney *et al.,* 2016, 2017) or the effects of refraction (García Muñoz *et al.,* 2012; Bétrémieux and Kaltenegger, 2013, 2014; Misra *et al.,* 2014b), this technique is generally most sensitive to the upper tropospheres and stratospheres of terrestrial planets, where our O_2 is still highly abundant. This gives O_2 an advantage over other proposed, often more complex biosignature molecules, including methanethiol, dimethyl disulfide (*e.g.,* Pilcher, 2003; Domagal-Goldman *et al.,* 2011; Seager and Bains, 2015), which are more susceptible to photolysis by UV radiation and so are confined largely to the lower troposphere, with significantly smaller concentrations in the stratosphere, which are less likely to be detectable (Domagal-Goldman *et al.,* 2011). Some organic molecules that could act as alternative biosignatures, such as ethane, may also resist photolytic destruction and be evenly mixed throughout the atmosphere (Domagal-Goldman *et al.,* 2011). Other more speculative biosignatures, such as NH_3 in oxidizing atmospheres as a disequilibrium biosignature (Lovelock, 1975) and NH_3 in H_2-dominated atmospheres (Seager *et al.,* 2013a, 2013b), may have to contend with NH_3 being susceptible to being dissolved in an ocean or destroyed by photolysis (*e.g.,* Pavlov *et al.,* 2001). However, in H_2-dominated atmospheres NH_3 may be more detectable in transmission due to the larger scale-height (Seager *et al.,* 2013b). Both ethane and ammonia have their strongest features in the MIR (near 13 and 9 μm, respectively; Rothman *et al.,* 2013), and sufficiently sensitive spectra of terrestrial planet atmospheres may be difficult to obtain at these wavelengths using transmission with the James Webb Space Telescope (JWST; Arney *et al.,* 2017). The MIR wavelength region is also not currently under consideration for future spaceborne exoplanet direct imaging telescopes (Dalcanton *et al.,* 2015), although it may be accessible to ground-based telescopes for very nearby planetary systems (Males *et al.,* 2014; Snellen *et al.,* 2015).

Although a single atmospheric species like O_2 can be considered a good biosignature, a combination of gases in chemical thermodynamic disequilibrium is considered even more robust (*e.g.,* Lederberg, 1965; Lovelock, 1965, 1975; Hitchcock and Lovelock, 1967). In chemical thermodynamic equilibrium, a mixture of gases is stable and will not react further. If atmospheric gases are seen in chemical disequilibrium, then this implies either an active planetary—possibly biological—source of the reactant gases, or the action of photochemistry. Once a chemical disequilibrium is identified, it is important to first rule out abiotic planetary processes as a source. The classic disequilibrium signature of life has been the simultaneous presence of both oxygen and methane in Earth's atmosphere, with a methane abundance that is many orders of magnitude above the equilibrium value (Lovelock, 1975; Sagan *et al.,* 1993). In chemical equilibrium these molecules would react, via formation of OH molecules from H_2O and O_3 photolysis, to form CO_2 and H_2O (*e.g.,* Segura *et al.,* 2005). Their disequilibrium implies active sources of both gases, which on Earth include photosynthetically generated O_2, and CH_4 from methanogenic bacteria and archaea, which outproduce geologically generated methane from serpentinization (Kelley *et al.,* 2005; Guzmán-Marmolejo *et al.,* 2013) and other water/rock reactions by at least a factor of

25 (Kasting and Catling, 2003; Kharecha *et al.,* 2005; Etiope and Sherwood Lollar, 2013). Another proposed disequilibrium biosignature is the combination of O_2 from photosynthesis and N_2O from bacterial denitrification (Lovelock, 1975). Like CH_4, biological sources of N_2O on Earth outproduce possible abiotic sources (Stein and Yung, 2003), of which several have been identified (Zhu-Barker *et al.,* 2015). These include chemodenitrification via brine/rock reactions in hypersaline environments, as observed in the Antarctic Dry Valleys (Samarkin *et al.,* 2010; Peters *et al.,* 2014); photolysis of nitrate ions in soils, an abiotic effect that may also show a seasonal signal (Rubasinghege *et al.,* 2011); or photochemical oxidation of atmospheric NH_3 (Stein and Yung, 2003). It has also recently been postulated that coronal mass ejections from the early Sun may have allowed energetic particles to drive the formation of N_2O on the early Earth via destruction of N_2 and CO_2 in the upper atmosphere (Airapetian *et al.,* 2016). However, the O_2/CH_4 and O_2/N_2O disequilibrium biosignatures were identified by considering only the composition of Earth's atmosphere, without considering the significant fraction of atmospheric gases that are dissolved in the ocean and undergo aqueous reactions. When the atmosphere/ocean system is considered, Earth's strongest disequilibrium biosignature is the simultaneous presence of abundant atmospheric O_2 and N_2 with an ocean, rather than a nitrate-rich ocean—which would be the equilibrium state (Krissansen-Totton *et al.,* 2016).

These disequilibrium biosignatures are potentially observable, although the O_2/N_2/ocean is perhaps the most challenging. O_2 and CH_4 may be detectable in a visible to NIR transmission or direct imaging spectrum of an exoplanet's atmosphere, or as the O_3 (9.6 μm)/CH_4 (7.7 μm) pair in the MIR. N_2O has strong features in the MIR, so the O_3 (9.6 μm)/N_2O (8.5 μm) pair would be the most diagnostic, although N_2O also absorbs, albeit more weakly, in the NIR at 2.11 and 2.25 μm (Rothman *et al.,* 2013). For modern Earth, both the N_2O and CH_4 abundances are low, at 0.3 and 1.8 ppm, respectively. Consequently, these disequilibria may have been more detectable during Earth's Proterozoic period, when the lower O_2 abundance could still generate potentially detectable O_3 yet also allow CH_4 to exist at higher atmospheric abundances than is currently possible (Segura *et al.,* 2003; Meadows, 2005; Kaltenegger *et al.,* 2007). Similarly, an N_2O-rich atmosphere may have formed during the Proterozoic due to the biological unavailability of Cu in a strongly sulfidic ocean. The dearth of Cu would have inhibited the final step of the denitrification process and preferentially released N_2O—rather than N_2—into the planet's atmosphere (Buick, 2007).

These disequilibria could also become more detectable for terrestrial planets orbiting M dwarfs, when compared to Earth-Sun analogues. For an M dwarf host, the slope of the UV spectrum of the star can alter photochemistry to extend the atmospheric lifetimes, and therefore the abundance, of both CH_4 and N_2O in the planetary atmosphere, given an Earth-like surface flux of these gases (Segura *et al.,* 2005; Grenfell *et al.,* 2012, 2014; Rugheimer *et al.,* 2015). In the case of CH_4, the UV spectrum of the star is less effective at photolyzing ozone to produce $O(^1D)$, thereby slowing the production of the OH radical from H_2O and inhibiting the destruction of CH_4 (Segura *et al.,* 2005). For N_2O, atmospheric buildup occurs because the M dwarf produces less radiation that would directly photolyze N_2O (<220 nm), when compared with a G dwarf (Segura *et al.,* 2005).

For the O_2/N_2/ocean disequilibrium biosignature, a surface ocean might be sought by using reflective "glint" from the ocean in the planet's phase-dependent photometry at visible to NIR wavelengths (Williams and Gaidos, 2008; Robinson *et al.,* 2010, 2014; Zugger *et al.,* 2011; Cowan *et al.,* 2012) while the oxygen could be sought as either O_2 or O_4 in the visible or NIR (Misra *et al.,* 2014a; Schwieterman *et al.,* 2016a, 2016b). N_2 could be searched for in the 80–100 nm region of the UV, or via N_4 absorption near 4.1 μm (Schwieterman *et al.,* 2015b). Uniquely identifying N_2 in the UV may be difficult without both an EUV-capable telescope and a relatively high spectral resolution—as the UV contains broad, overlapping bands from many atmospheric species. Alternatively, atmospheric N_2 may be sought near 4.1 μm via N_4 (also written as N_2-N_2) collisional absorption from pairs of N_2 molecules (Lafferty *et al.,* 1996), which overlap, but can be distinguished from, the 4.2 μm CO_2 absorption band in Earth's atmosphere (Schwieterman *et al.,* 2015b). However, the longer wavelength of the N_4 absorption will make these observations more challenging than the detection of Earth-like levels of O_2 for first-generation exoplanet characterization missions that will observe in the visible and/or NIR. To detect N_4, future direct imaging missions would need a significantly more expensive, cooled telescope to observe wavelengths as long as 4.2 μm. Similarly, JWST has less sensitivity for exoplanet transmission spectra at these longer wavelengths, due to increasing thermal background and the drop in stellar brightness.

3. Oxygen Biosignature False Positives

O_2 has long been considered the most robust biosignature possible, because there were no known "false positives." In this context, a false positive is an abiotic planetary process—such as volcanism or photochemistry—that could produce large, Earth-like quantities of O_2 on a habitable planet (*e.g.,* Rosenqvist and Chassefière, 1995). On Earth, the abiotic production of O_2, principally by photolysis of water vapor, is at least a million times less than that produced by photosynthesis (Walker, 1977; Harman *et al.,* 2015). Initial modeling results attempting to identify false-positive mechanisms concentrated on photolysis of CO_2 as a possible source of abiotic O_2. Rosenqvist and Chassefière (1995) used a steady-state photochemical model, and neglected surface sinks, to show that carbon dioxide–dominated abiotic atmospheres would produce an O_2 partial pressure of no more than 5 mbar (<600 ppm for the atmospheres modeled). Selsis *et al.* (2002) showed that for warm, ocean-bearing planets with 1 bar CO_2 atmospheres, O_2 could build up to only 1/10 of Earth's 21% present atmospheric level (PAL). However, even this relatively small amount was only possible if strong sinks for O_2 were neglected. These sinks include volcanic outgassing of reduced compounds, redox balance at the surface, and rainout of oxidized species, like H_2O_2. The latter mechanism acts as an O_2 sink because oxidized gases can react with reduced species in the crust or seawater to produce a net flux of H_2, which reacts with and removes the O_2. Segura *et al.* (2007) revisited the possible photolytic production of abiotic O_2 in CO_2-rich atmospheres with the three O_2 sinks discussed above included. They explored whether a CO_2-rich (up to 2 bar) atmosphere irradiated with strong incident UV from a

young Sun-like star (EK Dra; G1.5V)—a best-case scenario for CO_2 photolysis—could generate detectable levels of O_2. However, with the sinks in place, their models returned O_2 abundances that were typically less than 1 ppb in the troposphere. Later, Hu *et al.* (2012) explored abiotic generation of O_2 on potentially habitable planets assuming no volcanic outgassing, but with rainout of oxidized species included, and achieved an abundance of only 5×10^{-3} PAL (0.1% abundance), which is also highly unlikely to be detectable. When more realistic assumptions of volcanic outgassing were used, their O_2 abundances dropped to a few parts per million. As another possible abiotic mechanism for O_2 buildup, Léger *et al.* (2011) discussed the efficacy of known catalysts for abiotic photogeneration of O_2 from water-splitting on a planetary surface but concluded that it was highly unlikely to occur on a habitable planet, although a subsequent study argued that this may be possible, if significantly large areas of the planet supported a catalyst (Narita *et al.,* 2015). Another possible mechanism, O_2 derived from the release of H_2O_2 during the melt of a pole-to-pole ice-covered Snowball Earth (Liang *et al.,* 2006), also only produces abundances of a few parts per million of O_2 in the lower atmosphere.

3.1. False positives for oxygen and ozone on uninhabitable planets

Although buildup of significant amounts of abiotic O_2 or O_3 on habitable planets was initially precluded, it was thought more likely to occur on some uninhabitable planets. Mars and Venus have only small quantities of O_3 in their atmospheres, due to photolytic reactions with CO_2 (Blamont and Chassefière, 1993; Fast *et al.,* 2009; Montmessin *et al.,* 2011; Villanueva *et al.,* 2013). However, a terrestrial planet undergoing a runaway greenhouse or a frozen Mars-like planet beyond the outer edge of the habitable zone could both build up large amounts of O_2, and possibly O_3, in their atmospheres (Schindler and Kasting, 2000). The runaway greenhouse state would evaporate the planetary ocean and modify the atmospheric temperature structure to allow water to permeate the planet's stratosphere, above any UV-protective ozone layer. Photolysis of the unprotected H_2O and the subsequent loss of hydrogen to space would allow atmospheric O_2 to accumulate (Ingersoll, 1969; Kasting, 1988). Subsequent buildup of stratospheric O_3 would be delayed until the odd H from water photolysis had been lost to space (Schindler and Kasting, 2000; Leconte *et al.,* 2013). For a dry terrestrial planet beyond the outer limit of the habitable zone that was large enough to retain heavier gases, but too small or too old to maintain volcanic outgassing, the available sinks for O_2 would be small. Surface ice would preclude reactions with a reduced surface, and the lack of reduced gases from volcanic outgassing would allow O_2 from photolysis of H_2O or CO_2 to accumulate in the planetary atmosphere. The martian atmosphere today contains 0.1% O_2, and Mars may have built up more O_2 if it had been more massive and therefore resistant to O_2's atmospheric loss (McElroy, 1972).

Hot sub-Neptune planets may also form O_2-rich atmospheres when they are closer to the star than the habitable zone. Simulations of thermochemical and photochemical equilibrium states for hot (radiative equilibrium temperatures from 500 to 2000 K) super-Earth/mini-Neptune planets as a function of atmospheric hydrogen fraction and carbon-to-oxygen ratio do generate O_2-rich atmospheres in some cases (Hu and Seager, 2014). Specifically, these simulations show that planets with hydrogen fractions below about 50%, and with C/O ratios <0.1, form O_2-rich atmospheres of at least 20% O_2 (Hu and Seager, 2014, their Fig. 7). However, these hot sub-Neptunes would also display very high fractions of water vapor (from 1% to 60%) that would persist to high altitude (Hu and Seager, 2014) and potentially be visible to transit spectroscopy. This would help discriminate them from habitable Earth-like planets, which have water in the troposphere but relatively dry stratospheres, that would produce weak or no water vapor features in transmission.

Consequently, identifying known false positives for oxygen on planets not within the habitable zone may be relatively straightforward if the planet's orbit—and possibly size or mass—is known and the spectral range encompasses absorption from H_2O as well as O_2 and O_3. Such a planet will be outside or very close to the conservative habitable zone boundaries for its mass and atmospheric characteristics (Kopparapu *et al.,* 2013, 2014) and, if showing the abundant O_2 of a recent runaway or a hot Neptune, will also exhibit strong stratospheric H_2O, but no O_3 in either transmission or direct detection spectra. In the case of the planet beyond the outer edge of the habitable zone with abundant O_2, and for an older runaway greenhouse atmosphere close to the star that also exhibits both O_2 and a large O_3 component, water vapor will instead be weak or nonexistent in transmission or direct imaging spectra (Schindler and Kasting, 2000).

3.2. New false positives for oxygen and ozone on habitable zone planets

The recent identification of multiple mechanisms for abiotic generation of atmospheric oxygen or ozone for planets in the habitable zone presents a far more serious challenge to the robustness of oxygen as a biosignature. In many cases, water vapor, an extremely common molecule—and one hoped to be abundant on a habitable planet—serves as the key source of abiotic oxygen. Several of these false-positive mechanisms are more likely on planets orbiting in the habitable zones of M dwarf stars (Domagal-Goldman and Meadows, 2010; Domagal-Goldman *et al.,* 2014; Tian *et al.,* 2014; Gao *et al.,* 2015; Harman *et al.,* 2015; Luger and Barnes, 2015), but at least one mechanism could operate for planets orbiting in the habitable zones of stars of any spectral type, including G dwarfs (Wordsworth and Pierrehumbert, 2014). Photochemistry plays a significant role in all of these mechanisms and can leave telltale signs of its role in forming abiotic oxygen or ozone in the planetary atmosphere. By exploring these mechanisms and identifying the conditions under which they are most likely to occur, we will improve our interpretation of the spectra of habitable planets and be able to increase our confidence in life detection on exoplanets. In particular, we can improve target selection for the search for life on exoplanets by determining the stellar or planetary characteristics that increase the likelihood of abiotic O_2 or O_3 production, and identify the specific measurements required to discriminate between biological and abiotic production of O_2 and O_3.

3.2.1. Low noncondensable gas inventories.

The possible abiotic O_2 generation mechanism that will likely be the

most difficult to recognize involves photolysis of water—and subsequent hydrogen loss—from terrestrial atmospheres that are depleted in noncondensable gases (Wordsworth and Pierrehumbert, 2014). Because this mechanism relies primarily on a planetary property, the lack of atmospheric gases that will not condense at typical terrestrial planetary temperatures and pressures (*e.g.,* N_2 or O_2), this mechanism may work for planets orbiting stars of any spectral type, including Sun-like stars. In this proposed mechanism, the ''cold trap''—the rapid reduction in temperature with altitude that causes rising water vapor on Earth to condense and thereby remain trapped in the troposphere—is no longer effective. This can occur either when the atmospheric temperature is high or when the inventory of noncondensable gases—for example, N_2 or Ar—is low. In these cases, water rises into the stratosphere, where it is more vulnerable to photolysis by incident stellar UV radiation. The resultant H atoms escape, leaving oxygen to build up abiotically in the atmosphere. This continues until O_2, itself a noncondensable gas, reaches a sufficiently high abundance that it is able to establish a cold trap and halt the loss of water vapor.

Wordsworth and Pierrehumbert (2014) describe the relationship between surface temperature and surface partial pressure of noncondensable gas that determines whether a planet is more likely to have a moist upper atmosphere or one that remains dry. For 1 bar of N_2 in an N_2-H_2O atmosphere, a surface temperature >340 K would be required to produce a moist upper atmosphere. Conversely, for Earth's current surface temperature, a reduction in our current N_2 partial pressure by a factor of ~ 10 would be enough to move a planet into the moist upper atmosphere regime, where it would be susceptible to water loss and abiotic O_2 buildup (Wordsworth and Pierrehumbert, 2014). Interestingly, even though the Archean Earth's troposphere likely contained very little oxygen, there is recent evidence from preserved micrometeorites that the stratosphere of the Archean contained oxygen in abundances similar to modern Earth's, as might possibly have been formed by a water-rich stratosphere that was undergoing photolysis (Tomkins *et al.,* 2016).

Terrestrial exoplanets with different N_2 inventories are entirely plausible, and the delivery and loss of volatiles from a terrestrial planet are dependent on a number of planetary and exogenous processes that will be difficult to know *a priori*. In our own solar system, Mars and Venus have smaller (2×10^{-4}) and larger (3.3 times) atmospheric nitrogen abundances than Earth (Mancinelli and Banin, 2003; Hunten, 1993), with Venus' water loss and subsequent oxidation of the mantle potentially enhancing the outgassing of N_2 (Wordsworth, 2016). Hydrodynamic escape during the pre-main sequence phase of M dwarfs may also lead to atmospheric N_2 loss. Recent modeling estimates for Proxima Centauri b, a possibly terrestrial planet with a minimum mass of 1.3 $M_\oplus$ orbiting an M5.5V star (Anglada-Escudé *et al.,* 2016), suggest that less than a bar of N_2 may be lost this way in the first 100 million years (Ribas *et al.,* 2016).

Earth may have also exhibited different N_2 partial pressures throughout its history, as its atmosphere evolved. Paleobarometry measurements of 2.7 Ga fossilized raindrop imprints indicate that Earth's atmospheric pressure was no more than twice the modern day's but potentially as low as 0.5 bar (Som *et al.,* 2012). Subsequent analyses of nitrogen and argon isotopes in 3.5 Ga rock (Marty *et al.,* 2013) showed a similar range of 1.1–0.5 bar for the partial pressure of N_2 in the ancient atmosphere. Som *et al.* (2016) used the distribution of sizes in gas vesicles in 2.7 Ga volcanic rocks to derive an atmospheric pressure of 0.23 ± 0.23 bar, which when combined with the previous studies suggested that 0.5 bar was a likely upper limit to the atmospheric pressure in Earth's Archean.

For an abiotic planet that is largely Earth-like except for the N_2 inventory, this proposed mechanism could result in a planet that nonetheless exhibited a very Earth-like O_2 partial pressure, while losing significant amounts of water. A pure water vapor atmosphere would initially be susceptible to water loss and O_2 buildup, until the (noncondensable) O_2 constituted a large enough fraction of the atmosphere to produce a cold trap for the water vapor. Under the assumption of redox balance—with loss of hydrogen to space balanced by the surface removal rate of oxidizing material for an Earth-like (288 K surface temperature) planet—the resultant atmospheric fraction of O_2 was found to be 0.15 bar (Wordsworth and Pierrehumbert, 2014). However, this amount of O_2 could be higher or lower, depending on surface and tropopause temperatures. In the case of a more Earth-like atmosphere containing N_2-H_2O and sufficient CO_2 to produce our current surface temperature, once the N_2 content drops significantly, to below a few percent of Earth's current levels, the upper atmosphere becomes rich in H_2O and susceptible to hydrogen loss and O_2 buildup. If this process persists for 4 billion years around a Sun-like star—and the resultant O_2 is absorbed by the planet's surface and interior, instead of building up in the atmosphere and shutting off the water loss—then as much as a third of an Earth ocean could ultimately be lost from the planetary environment. Even higher water loss rates are expected for stellar XUV fluxes higher than the Sun's current flux (Wordsworth and Pierrehumbert, 2014), as might be expected for planets orbiting F dwarfs and active M dwarfs (*e.g.,* France *et al.,* 2016; Fig. 1).

3.2.2. Enhanced pre-main sequence stellar luminosity. Another recently proposed mechanism to generate high levels of abiotic oxygen, first proposed by Luger and Barnes (2015), focuses on the effects of the pre-main sequence, superluminous phase of young stars on terrestrial planet environments Before settling in to their main sequence hydrogen-burning phase, young stars can be significantly more luminous due to additional energy production from their extended contraction phase (*e.g.,* Baraffe *et al.,* 1998), so planets that form in what will become the main sequence habitable zone are subjected to very high levels of radiation early on (Lissauer, 2007). This superluminous phase is most pronounced—and of longer duration—for smaller-mass M dwarfs than for any other stellar spectral type, where it can extend for up to 1 billion years (Baraffe *et al.,* 1998). Modeling suggests that during this superluminous phase a terrestrial planet that forms within what will become the main sequence habitable zone around an M dwarf star may lose up to several Earth ocean equivalents of water due to evaporation and hydrodynamic escape, and this can lead to generation of large amounts of abiotic O_2 (Luger and Barnes, 2015; Tian, 2015). This superluminous phase may persist for 200 million years or more for M dwarf stars of less than 0.4 $M_\odot$ (M3V and later; Baraffe *et al.,* 1998). The resultant water-rich atmosphere will be susceptible to

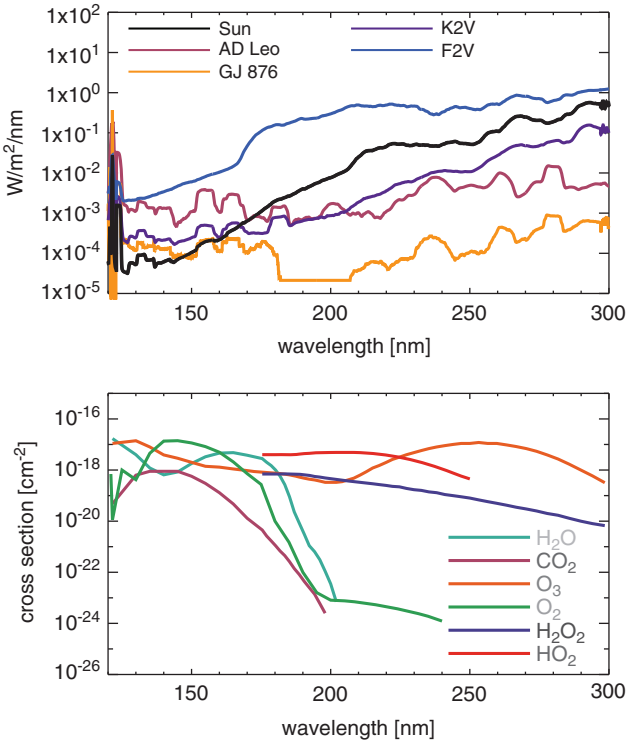

FIG. 1. Comparison of stellar UV fluxes and molecular absorption cross sections. The upper panel shows the UV fluxes for a range of stellar types, including the two M dwarf stars AD Leo (M3.5V) and GJ 876 (M4V). The lower panel shows the UV absorption cross sections for oxygen and ozone, as well as several key molecules involved in the abiotic production of oxygen and ozone. Because the stellar UV spectra have different slopes, and the molecules have different regions of the UV spectrum in which they absorb radiation and can potentially be photolyzed, stellar spectral slopes can drive the formation or destruction of abiotic oxygen and ozone. (Credit: G. Arney)

photolysis and hydrogen escape, thereby producing potentially hundreds or thousands of bar of O_2 (Luger and Barnes, 2015) as photolysis of an Earth ocean of water can result in ~240 bar of O_2 (Kasting, 1997). The amount of O_2 generated is a strong function of several factors, including stellar spectral type, XUV flux, original water inventory, planetary mass, and the position of the planet in the habitable zone. Planets in the outer regions of the habitable zone for M0–M3V stars are the least likely to generate significant amounts of abiotic O_2 (Luger and Barnes, 2015), along with M1–M3V dwarfs with lower stellar XUV, as slower water loss may preclude O_2 generation and buildup (Tian, 2015). However, for planets orbiting later type M dwarfs (M4V and later), depending on the planet's original water inventory, mass, stellar parameters, and the strength of surface sinks (Rosenqvist and Chassefière, 1995; Schaefer *et al.,* 2016), several Earth ocean equivalents of water, or up to several hundreds of bar of photolytically produced O_2, could plausibly build up in the atmospheres of these planets (Luger and Barnes, 2015). For the recently discovered Proxima Centauri b, orbiting an M5.5V star, estimates for maximum ocean loss during the pre-main sequence phase span less than one ocean, assuming a constant XUV flux for the host star for the first 3 billion years (Ribas *et al.,* 2016), to 3–10 oceans lost, assuming that the XUV scales with the decreasing bolometric luminosity (Barnes *et al.,* 2016).

Note also that this mechanism for O_2 production and buildup relies on water loss being shut down within 1 billion years of planet formation, when the host star joins the main sequence and dims in luminosity and the habitable zone sweeps in to encompasses the planet. For planets that form much closer to the star than the main sequence habitable zone, and do not enter the habitable zone during the star's lifetime, hydrodynamic escape and subsequent loss of photolytically produced O_2 can be enhanced. Schaefer *et al.* (2016) modeled this scenario for GJ 1132b, a 5-billion-year-old 1.2 Earth radii planet that is currently still closer to its star than the habitable zone (Berta-Thompson *et al.,* 2015). Schaefer *et al.'s* XUV Model A is comparable to that used by Luger and Barnes (2015), yet their simulations showed that as the planet's total amount of water decreased over 5 billion years, the ratio of O_2 escape to O_2 production from water photolysis increased, driving the planet toward states with no more than a few bar of O_2 and H_2O remaining (Schaefer *et al.,* 2016). For these "hot Earths," they concluded that hundreds to thousands of bar of O_2 could persist only for planets with very large initial water abundances of >5% wt %, which over 5 billion years would never be sufficiently depleted in water to get to the O_2 escape "runaway" scenario. However, as Luger and Barnes (2015) and Barnes *et al.* (2016) show, a planet that enters the habitable zone prior to 1 billion years can also shut down hydrodynamic escape and avoid massive O_2 loss and could do so with water abundances significantly lower than 5% wt %.

Once they enter the habitable zone, these M dwarf planets with O_2-rich atmospheres may be completely desiccated, or could still support a surface ocean, especially if the superluminous phase ends before the runaway process is complete (Luger and Barnes, 2015; Barnes *et al.,* 2016). Water may also be delivered after the superluminous phase is complete, although in the case of M dwarfs the billion-year superluminous phase will significantly exceed the up to several million-year timescales for planet formation, and the majority of volatile delivery (Raymond *et al.,* 2008). Volatile outgassing from the mantle may be another way to form a surface ocean. However, in the case of Earth, noble gas analysis suggests that the vast majority of our volatiles (80–95%) outgassed within the first 500 million years (Turner, 1989). An ocean of water may have remained in the mantle after this initial loss (Albarède, 2009; Sleep *et al.,* 2012), and it is being more slowly outgassed. If a similar process works for terrestrial planets orbiting M dwarfs, then these planets would be susceptible to significant loss of mantle-outgassed water during the pre-main sequence phase. However, under favorable conditions a terrestrial planet could perhaps, over billions of years, slowly accumulate a surface ocean from outgassed water, after the M dwarf has settled into its more benign main sequence phase. Conversely, if the mantle is desiccated during the extended pre-main sequence phase, then the development of a later ocean may be stymied. The lack of surface water and the inhibition of subduction, due to a lack of hydrated minerals, will severely limit the recycling of water back into the mantle for later release, as was possibly the case for the now largely desiccated Venus (Grinspoon, 1993; Hamano *et al.,* 2013).

3.2.3. Stellar spectrum–driven photochemical production. A perhaps more subtle mechanism for formation of abiotic

O_2 and its proxy, O_3, is planetary photochemistry In this context, photochemistry is primarily an interaction between molecules in a planetary atmosphere and the incident UV spectrum of the parent star, which can split molecules and drive reactions that change the composition of the atmosphere. Each photochemical reaction requires photons that exceed a threshold energy level—or equivalently, photons at wavelengths shorter than a threshold wavelength—to be absorbed by the molecule undergoing photolysis. Planetary photochemistry is therefore strongly sensitive to the UV spectral energy distribution of the parent star (*e.g.,* Segura *et al.,* 2003, 2005; Grenfell *et al.,* 2007, 2014; Rugheimer *et al.,* 2013, 2015), and in particular the ratio of shorter- to longer-wavelength UV radiation (Fig. 1).

In addition to the stellar UV radiation, the entire planetary environment can be involved in providing sources and sinks for the photochemical reactions. For example, photochemical abiotic O_2 production will depend strongly on the source of O atoms, which is primarily controlled by the photolysis rates of H_2O, CO_2, SO_2, and other O-bearing gases. Similarly, the atmospheric sink will depend on the availability of H atoms in the atmosphere from H_2 and H_2S. While water vapor can be sourced from a planetary ocean, the availability of other gases, such as CO_2, SO_2, and reducing (H-bearing) gases, is governed by the planet's volcanic outgassing rates, which can be sustainable on long geological timescales. CO_2 in particular is likely a common atmospheric gas on terrestrial planets. In our own solar system, CO_2 dominates the atmospheric composition on Mars and Venus and was likely a significant component of the early Earth's atmosphere as well (Kasting, 1993; Sheldon, 2006; Sleep, 2010; Driese *et al.,* 2011).

The photochemical production of O_2 is governed primarily by a few key photochemical reactions. CO_2 is photolyzed to produce CO and O atoms, by wavelengths of light shorter than 175 nm:

$$CO_2 + h\nu\ (\lambda < 175\ \text{nm}) \rightarrow CO + O$$

O released from this reaction or from similar reaction for other O-bearing gases may recombine to form O_2 via three-body reactions, and eventually O_3. The distribution of those O atoms between O_2 and O_3 is critical to the concentration of either species and is primarily controlled by four reactions known as the Chapman mechanism (Chapman, 1930):

$$O_2 + h\nu\ (\lambda < 240\ \text{nm}) \rightarrow O + O$$

$$O + O_2 + M \rightarrow O_3 + M$$

$$O_3 + h\nu\ (\lambda < 340\ \text{nm}) \rightarrow O_2 + O$$

$$O + O_3 \rightarrow O_2 + O_2$$

Here, $h\nu$ represents the photon energy for photons with wavelengths in the indicated range, and the M denotes a third molecule that does not participate in the reaction but only carries off excess energy. Note that although the Chapman mechanism dominates ozone production, other reactions, especially with oxygen-bearing species such as HO_x (*e.g.,* H_2O, OH), NO_x (*e.g.,* N_2O, NO, NO_2) and chlorine-bearing compounds can also affect O_2 and O_3 abundances (*e.g.,* Stolarski and Cicerone, 1974; Johnston, 1975; Thornton *et al.,* 2002). In CO_2- and O_2-rich atmospheres, these molecules can reduce O_2 and O_3 abundances by catalyzing CO_2 recombination (Domagal-Goldman *et al.,* 2014), although these molecules can react to generate O_2 in anoxic environments such as the early Earth, especially for planets orbiting stars with relatively high far-UV (FUV) fluxes (Arney *et al.,* 2017). The effects of these catalytic species on O_2 and O_3 abundances in planetary atmospheres are discussed in more detail below.

Concentrating on the direct photolytic effects described in the Chapman mechanism, the photolysis of CO_2 and O_2 requires FUV photons at wavelengths < 200 nm, and the process provides O atoms to help from O_2 and O_3. Balancing O_3 production, the photolytic destruction of O_3 is primarily driven by photons in the mid-UV (MUV: 200 nm < λ < 300 nm) but can also be achieved by photons in the near-UV (NUV: 300 nm < λ < 440 nm) and visible (~440 to 800 nm) (Sander *et al.,* 2006). Since CO_2-photolyzing FUV photons are produced by stellar activity (Pace and Pasquini, 2004) and O_3-photolyzing MUV-NUV and visible photons are primarily due to a star's blackbody radiation, then the spectrum and activity levels of the host star will strongly affect the balance between production and destruction of oxygen and ozone. Consequently, to interpret the atmospheric composition of terrestrial exoplanets, it will be extremely important to understand the UV spectrum of the host star, especially for the high-UV-output F and M dwarfs (*e.g.,* Hawley *et al.,* 2003; Walkowicz *et al.,* 2008 ; France *et al.,* 2012, 2016 ; Loyd *et al.,* 2016; Youngblood *et al.,* 2016). Because Ly α emission dominates M dwarf UV output and can photolyze CH_4, CO_2, and H_2O in the upper planetary atmosphere (>60 km in Earth's atmosphere), it may also be important to reconstruct the star's intrinsic Ly α (112 nm) profile by correcting the observed Ly α line for the effects of interstellar absorption (Wood *et al.,* 2005; Linsky *et al.,* 2013; Shkolnik *et al.,* 2014; Youngblood *et al.,* 2016).

The sinks for O_2 and O_3 are primarily controlled by the chemical context of the atmosphere and oceans, including the redox state of the atmosphere. As discussed above, these sinks include the destruction of O_2 and O_3 via direct photolysis but also include reactions with catalytic agents that can work to drive the recombination of O atoms with the parent molecule. On Earth, these include reactions with Cl and other halogens.

In anoxic atmospheres, the greatest sinks for O_2 and O_3 are reactions with reduced radicals in the atmosphere, such as

$$CH_3 + O_2 \rightarrow H_2CO + OH$$

When the concentration of reduced species such as CH_4 increases in the atmosphere, so do the concentrations of photolytically produced radicals such as CH_3, and these can react with O_2 and O_3, keeping their concentrations low. Major abiotic sources of reduced species include volcanic outgassing of H_2 and submarine production of CH_4 (Kelley *et al.,* 2005; Guzmán-Marmolejo *et al.,* 2013), and their sinks are primarily determined by the redox state of the atmosphere and oceans (Kharecha *et al.,* 2005; Domagal-Goldman *et al.,* 2014; Harman *et al.,* 2015).

In the absence of reduced radicals, the main counter to O_2/O_3 production by CO_2 photolysis would be recombination of

CO and O to form CO_2. However, the direct three-body recombination reaction for CO_2, which would remove O from the atmosphere,

$$CO + O + M \rightarrow CO_2 + M$$

is spin forbidden and proceeds extremely slowly. Consequently, catalysts are much more efficient at stabilizing CO_2 against photolysis in a planetary atmosphere. In particular, photolysis of water vapor ($H_2O + h\nu \rightarrow H + OH$) and HO_x chemistry can facilitate the recombination of CO_2 via the following reaction sequence:

$$H + O_2 + M \rightarrow HO_2 + M$$

$$O + HO_2 \rightarrow OH + O_2$$

$$OH + CO \rightarrow CO_2 + H$$

$$CO + O \rightarrow CO_2$$

Conversely, an atmosphere with low amounts of water vapor can accumulate higher amounts of O_2 and O_3—due to the slowdown of the catalytic recombination of CO_2.

In addition to reactions in the atmosphere, there is also a possible role for aqueous reactions in the ocean as sinks to remove atmospheric oxygen. For example, the aqueous reaction of dissolved CO and O_2 to reform CO_2 and draw down atmospheric oxygen is poorly understood but is crucial to understanding the final balance of O_2 in the atmosphere (Harman *et al.,* 2015). Similarly, weathering of surface crust (*e.g.,* Anbar *et al.,* 2007) and the sequestration of O_2 into the planetary mantle (*e.g.,* Schaefer *et al.,* 2016) are key processes that control O_2 drawdown and could result in abiotic O_2 buildup if weak. Conversely, if these processes are aggressive enough, they could instead result in a false negative for biologically produced O_2 by scrubbing photosynthetically generated O_2 from a planetary atmosphere. This may have been the case on our planet, where the evolution of oxygenic photosynthesis may have predated the rise of atmospheric oxygen by hundreds of millions to billions of years (Catling *et al.,* 2001; Catling and Kasting, 2007; Lyons *et al.,* 2014; Planavsky *et al.,* 2014a).

Several groups have explored these complicated, interacting factors and have found multiple mechanisms by which photochemical processes may generate abiotic O_2 and O_3 on terrestrial planets in the habitable zone (Domagal-Goldman and Meadows, 2010; Hu *et al.,* 2012; Domagal-Goldman *et al.,* 2014; Tian *et al.,* 2014; Gao *et al.,* 2015; Harman *et al.,* 2015). However, the amounts of abiotic O_2 and O_3 generated in these simulations differ, in part due to different assumptions about the ability of CO and O_2 to react in seawater.

Domagal-Goldman *et al.* (2014) used an altitude-dependent (1-D) photochemical model to perform an extensive parameter sweep through a wide variety of volcanic gas fluxes and stellar energy distributions to explore those conditions that could lead to abiotic O_2 and O_3 production. The approach used was conservative with respect to generation of O_2 and O_3 and included the enhanced boundary conditions needed for redox balance in the atmosphere and ocean. They assumed that a redox imbalance at the atmosphere-ocean interface would work to increase the ocean concentration of the species contributing to the redox imbalance. This allowed the aqueous CO and O_2 reaction to occur, serving as a strong sink for O_2. However, the increased concentration would ultimately slow down the rate the species dissolved into the ocean—as that rate is dependent on concentration—until an equilibrium was reached. Even with this conservative approach, Domagal-Goldman *et al.* (2014) still found that it was possible to generate abiotic ozone, primarily from the photolysis of CO_2, that was only a factor of 10 less than Earth's current ozone abundance. Small amounts of abiotic O_2, of the order of 40 ppm, significantly less than Earth's current 21% O_2 abundance, were also generated on these planets. This mechanism for abiotic O_3 generation was most likely to occur for habitable zone planets orbiting stars that have high FUV fluxes, as might be expected for F dwarf and active M dwarf stars, and for atmospheres that have high CO_2 concentrations and low H_2 concentrations (Domagal-Goldman *et al.,* 2014). This work demonstrated that O_3 could build up to potentially detectable levels, even if CO and O_2 can react in seawater. It also identified the environmental conditions associated with this false positive: high FUV fluxes from the host star, low CH_4 in the atmosphere, and high amounts of volcanic CO_2. Given that stellar UV output and volcanic sources of CO_2 and H_2 could be sustained for billions of years on a geologically active planet, this abiotic source of O_3 could be sustainable on similar timescales. Earlier work by Hu *et al.* (2012) had also been able to generate high levels of O_3 in CO_2-dominated atmospheres orbiting Sun-like stars using a similar mechanism, but only if the assumption of no volcanic outgassing was used. In that case, O_3 column abundances were only a factor of 3 lower than that on present-day Earth. When more realistic volcanic outgassing rates were used, however, the abundance dropped by 4 orders of magnitude.

Tian *et al.* (2014) used a 1-D photochemical model for a smaller array of cases, varying surface temperature and CO_2 mixing ratio (from 1% to 10%), to show that abiotic O_2 and O_3 could be generated around M dwarf stars that have FUV/NUV ratios significantly larger than the solar value. These researchers used HST observations of six planet-hosting M dwarfs (France *et al.,* 2012, 2013), showing that five of them are strong emitters at FUV wavelengths but weak emitters in the NUV. The remaining M dwarf emitted too little UV radiation to get a definitive measurement. The results of the photochemistry model showed buildup of O_2 in the atmosphere of a hypothetical planet orbiting GJ 876 to a mixing ratio of 0.2% (10^{-3} PAL) below 70 km. The authors argued that this is primarily due to the M dwarf's significantly weaker NUV compared to FUV flux, which slows the production of OH radicals (from photolysis of H_2O_2 and HO_2) that catalyze the recombination of CO_2 and the removal of atmospheric O_2. However, the absorption cross sections for the H_2O_2 and HO_2 molecules are not measured in the FUV (Fig. 1) and are unavailable to be included in photochemical models, so it is not clear what the action of the more abundant FUV radiation would be on the production of OH radicals from these molecules. Harman *et al.* (2015) instead argued that it is in fact decreased water vapor photolysis,

which slows by a factor of 400 for the GJ 876 case when compared to the solar case, coupled with the longer lifetimes of HO_2 and H_2O_2 that ultimately limits the availability of OH for the recombination of CO and O_2 in these atmospheres.

The lower boundary conditions may also lead to this O_2 buildup. In the Tian *et al.* (2014) model, surface CO and O_2 deposition velocities were set equal to each other, as the two molecules have similar diffusivities and solubilities in water. However, O_2 reacts much more strongly than CO with other constituents in the ocean, and O_2 would be preferentially removed from ocean water. This would increase the deposition rate of O_2 compared to CO and generate a net sink for O_2 that is not taken into account in this study. Also, although the O_2 may be generated by photochemistry in the stratosphere, it is the deposition rates at the lower boundary that control the vertical profile and column depth of the gas in the atmosphere (*e.g.,* see Fig. 3 in Harman *et al.,* 2015). Additionally, the highest O_2 and O_3 values modeled were associated with an assumption that CO and O_2 cannot recombine in seawater, which therefore assumes no aqueous sink for CO, as well. CO would also tend to accumulate in an atmosphere that could generate abiotic O_2, and act as a indicator for this photochemical mechanism.

Following on from Domagal-Goldman *et al.* (2014) and Tian *et al.* (2014), Harman *et al.* (2015) used a 1-D photochemical model to perform a comparison of abiotic O_2 from the photolysis of CO_2 on habitable planets with water oceans orbiting stars of different spectral types. Like Domagal-Goldman *et al.* (2014), they modeled systems with global redox balance between the ocean-atmosphere system, although they neglected oxygen sinks such as surface weathering. However, they simulated boundary condition limits for the deposition of CO and O_2 into the ocean (*i.e.,* insoluble and extremely soluble), to account for the uncertainly in the reaction rates for CO and O_2 in seawater. Harman *et al.* (2015) also defined an oxygen false positive not as something comparable to Earth's PAL but instead as being equivalent to the lower limit on the abundance of O_2 during the Proterozoic era of Earth's history, namely 10^{-3} PAL (Planavsky *et al.,* 2014b), or a mixing ratio of 0.02% O_2. They argued that this is the lower bound for a biologically produced O_2 concentration, although estimates of the Proterozoic O_2 abundance vary widely (*e.g.,* Kump, 2008; Lyons *et al.,* 2014). Harman *et al.* (2015) found that O_2 derived from CO_2 photolysis was significantly lower than 0.02% on planets around F- and G-type stars, although presumably O_2 concentrations in the atmosphere could be higher if background N_2 concentrations were unusually small and the planets had compromised cold traps (Wordsworth and Pierrehumbert, 2014). For planets orbiting a Sun-like star, the surface O_2 mixing ratio found by Harman *et al.* (2015) never rose above 10^{-13}, so they were not able to reproduce the relatively high surface O_2 concentrations (0.2%) obtained by Hu *et al.* (2012), even when using the unrealistic boundary condition of no H_2 outgassing. However, Harman *et al.* (2015) found that K dwarf and especially M dwarf planets may build up more significant amounts of abiotic O_2 because of the higher FUV/NUV flux ratio from their parent stars, similar to the results of Tian *et al.* (2014). This abiotic O_2 would be enhanced if recombination of dissolved CO and O_2 in the oceans is slow and if other O_2 sinks (*e.g.,* reduced volcanic gases or dissolved ferrous iron) are small. They posited a ''worst-case scenario'' where for each planet modeled the ocean was saturated with O_2, implying that both the deposition velocity and the rainout rate for O_2 were zero, and sink reactions could not occur in the ocean. For this scenario, their model generated an atmosphere with 6% O_2 (0.3 PAL) for an abiotic planet orbiting M dwarf GJ 876. When adopting more realistic boundary conditions, and also assuming that CO and O_2 react rapidly in solution, the column abundance of abiotic O_2 was a thousand times less. In keeping with Domagal-Goldman *et al.* (2014) and Hu *et al.* (2012), they also found that O_3 would be built up to potentially detectable levels at UV wavelengths for a much broader range of boundary conditions and stellar types.

Gao *et al.* (2015) also used a 1-D photochemical model to investigate whether CO_2-dominated atmospheres could remain chemically stable on terrestrial planets orbiting M dwarfs. Their mechanism relies on the planet being desiccated, so that water is not available to catalyze the recombination of CO_2 and the balance between CO_2 photolysis and recombination would instead be shifted toward production of large amounts of atmospheric O_2. In this case, the O_2 buildup for this habitable zone planet is also due to suppression of the catalytic recombination of $CO + O_2$ to form CO_2, but instead of the stellar FUV/NUV ratio driving the suppression of this cycle as proposed in Tian *et al.* (2014), it is inhibited by lack of atmospheric water vapor. We do not see this phenomenon on Earth, as our relatively high abundance of water vapor drives the catalytic recombination of CO_2 after photolysis. However, planets orbiting in the habitable zones of M dwarf stars may be depleted in water due to M dwarfs' prolonged, high-luminosity pre-main sequence phases (*e.g.,* Luger and Barnes, 2015) or may have formed volatile-poor (Lissauer, 2007; Raymond *et al.,* 2007). For these desiccated planets with atmospheric H mixing ratios <1 ppm, Gao *et al.* (2015) found that $\sim$40% of the atmospheric CO_2 was converted to CO and O_2 on a timescale of 1 million years, resulting in an atmosphere dominated by CO_2, CO, and O_2. However, the process did not destroy all the CO_2, as the increased O_2 abundance also led to high O_3 concentrations, and O_3 photolytic products form another CO_2-regenerating catalytic cycle. This catalytic cycle feedback places an upper limit of $\sim$50% on the CO_2 that can be destroyed via photolysis, but this is still enough to generate Earth-like abundances of abiotic O_2 and O_3. Specifically, a 90% CO_2 atmosphere with a total hydrogen mixing ratio of a few parts per million equilibrated at a concentration of 50% CO_2, 30% CO, and 15% O_2 (with the remainder being N_2), producing a similar oxygen fraction to that seen in Earth's current atmosphere (Gao *et al.,* 2015). If desiccated, CO_2-rich planets are common in the habitable zones of M dwarfs, then the abiotic conditions that lead to such high oxygen levels could be common also.

3.2.4. Summary and discussion of abiotic generation of O_2 and O_3. In aggregate, this research indicates that there are several mechanisms that could produce abiotic O_2 and O_3 in a planet's atmosphere, with each presenting a potential false positive to different degrees. A summary of this information is presented in Table 1. Two of the mechanisms allow water to enter a planet's stratosphere where it is

Table 1. Summary of Known Abiotic O_2 Generation Mechanisms

Mechanism	*Action*	*Targets affected*	*Potential O_2 produced*	*Potential O_3 produced*	*Spectral discriminant*	*References*
O_2 runaway from a superluminous pre-main sequence star	Massive H_2O evaporation and photolysis during the host star's superluminous pre-main sequence phase	HZ planets orbiting late-type M dwarfs	100s of bar, depending on initial water inventory	Possible, after complete loss of H_2O	O_4 in transmission (NIR) and direct imaging (visible + NIR)	Luger and Barnes, 2015; Tian, 2015
Lack of noncondensable gases	Lack of cold trap allows water to enter stratosphere and be photolyzed	HZ planets orbiting any stellar type	15% O_2	Not calculated	Quantification of O_2, and N_2 abundance via the N_2-N_2 collisional pair at 4.1 μm	Wordsworth and Pierrehumbert, 2014
Desiccated planets	Lack of water inhibits catalytic recombination of CO_2	HZ planets orbiting late-type M dwarfs, also volatile-poor planets	15% O_2	0.2 times Earth's for M dwarfs	Absence of H_2O absorption in direct imaging. O_3 looks similar to Earth's.	Gao *et al.,* 2015
Photochemical production from CO_2 photolysis	High stellar FUV/NUV, reduction of O_2 sinks	HZ planets orbiting K and M dwarfs	<0.02% for F and G star planets <6% for M dwarf planets with O_2-saturated oceans	0.15–0.01 times Earth's for M dwarf planets depending on sinks	Presence of CO, CO_2, M dwarf spectral host	Harman *et al.,* 2015
Photochemical production on CO_2-rich, H-poor planets	High stellar FUV/MUV photolysis CO_2 and produces O_3	HZ planets orbiting F dwarfs and some M dwarfs	40 ppm	0.1 times Earth's for M dwarfs	Presence of CO, absence of H-bearing gases such as CH_4	Domagal-Goldman *et al.,* 2014
Photochemical production from CO_2 photolysis and stellar inhibition of recombination	High stellar FUV/NUV destroys HO_x species and inhibits CO_2 recombination	HZ planets orbiting M dwarfs, CO_2-rich (<10%) atmospheres	0.2% for M dwarfs with high FUV/NUV ratios	0.06 times Earth's for M dwarfs	Presence of CO, CO_2, high FUV/NUV ratio for the parent star with low absolute NUV	Tian *et al.,* 2014
Photochemical production from CO_2 photolysis	CO_2 photolysis and no CO_2 or CH_4 surface flux	1 bar CO_2-rich (90%) atmospheres orbiting a G2V	0.1% O_2	0.3 times Earth's for G dwarfs	Presence of CO, CO_2	Hu *et al.,* 2012

HZ = habitable zone.

photolyzed, and the H atoms lost to space, resulting in O_2 buildup in the planet's upper atmosphere. Water entering the stratosphere is either enabled by loss of an ocean in a runaway greenhouse process (Luger and Barnes, 2015)—a mechanism that is most effective for late-type (*i.e.,* less massive) M dwarfs—or via lack of noncondensable gases in the planetary atmosphere, which could affect planets orbiting stars of any spectral type (Wordsworth and Pierrehumbert, 2014). The runaway mechanism could produce an O_2-dominated atmosphere of hundreds of bar, and the lack of noncondensable gases could potentially result in atmospheres that are $\sim$15% O_2. The other major class of processes that build up abiotic O_2 relies on the photolysis of CO_2 and circumstances that inhibit CO_2 recombination from CO and O_2 (Hu *et al.,* 2012; Tian *et al.,* 2014; Gao *et al.,* 2015; Harman *et al.,* 2015). In the mechanism that could potentially produce the largest signal from CO_2 photolysis, a desiccated, cold, hydrogen-poor atmosphere inhibits the CO_2 recombination reaction due to lack of photolytic generation of the OH catalyst from water (Gao *et al.,* 2015). A catalytic cycle feedback with ozone formation may result in stable atmospheric fractions of O_2 near 15%. It has also been proposed that recombination of photolyzed CO_2 can be slowed by a parent star with a higher FUV ($\lambda < 200$ nm) to MUV and NUV (200 nm $< \lambda <$ 440 nm) ratio when compared to the Sun, as the higher FUV photolyzes CO_2, but the lower MUV-NUV radiation inhibits the photolysis of water and other HO_x chemistry that would drive recombination (Tian *et al.,* 2014; Harman *et al.,* 2015). For the cases considered for this mechanism, O_2 abundances as high as 0.2% to 6% are predicted, with higher values corresponding to little or no O_2 sinks in the planetary environment. When more realistic sinks are included, abiotic O_2 abundances are reduced by many orders of magnitude (*e.g.,* Harman *et al.,* 2015). Abiotic O_3 buildup can occur via photolysis of abiotic O_2, with calculated values ranging from 1% to 30% of Earth's current ozone abundance. However, O_3 could also be photochemically generated as a result of the spectral slope of the UV radiation of the star, even without buildup of O_2. FUV radiation can favor the generation of ozone via photolysis of CO_2 (and O_2), whereas MUV or NUV radiation photolytically destroys O_3. Consequently, abiotic O_3 could accumulate—even without significant generation of O_2—for stars with the highest FUV to MUV ratios. O_3 was produced at 10% of Earth's current O_3 column abundance in the simulations of Domagal-Goldman *et al.* (2014) for M dwarf planets, without appreciable buildup of abiotic O_2. Although these mechanisms to generate abiotic O_2 and O_3 are driven primarily by the interaction of the incident stellar spectrum with the planetary atmosphere, they can be balanced by the destruction or sequestration of O_2 and O_3 in the planetary environment. These losses could be via photolysis, catalytic recombination into CO_2, or interaction with the planetary surface and ocean, if present. The net atmospheric accumulation of O_2 and O_3 is highly sensitive to these boundary conditions, which include weathering rates, and aqueous sinks for CO, all of which are currently poorly understood.

Venus, for example, appears to stand as a sobering counter example for abiotic O_2 production, as its postrunaway, mostly desiccated, high-CO_2 atmosphere is currently undergoing rapid photolysis—yet Venus does not exhibit a high atmospheric abundance of abiotic O_2 or O_3. The modern venusian atmosphere is extremely hydrogen poor, with only about 30 ppm of water vapor below its cloud deck (Meadows and Crisp 1996; Arney *et al.,* 2014), and about 2–5 ppm of H_2O above it (Cottini *et al.,* 2012), with the other principal H-bearing gases, HF and HCl, found at abundances much less than 1 ppm (Krasnopolsky, 2010). Venus may have been wetter in the past but likely underwent a catastrophic runaway greenhouse, and the observed enhancement in its atmospheric D/H ratio suggests that Venus lost a global ocean of at least 3 m in depth (De Bergh *et al.,* 1991). This is a lower limit, and Venus' ocean could have been significantly larger—as the D/H ratio may not record hydrodynamic escape, where heavier molecules are removed along with the lighter hydrogen (Chassefière, 1996b). Taking into account hydrodynamic H and O loss, along with likely surface and mantle sinks for O_2, Chassefière (1996a) calculated that Venus could only have avoided developing an O_2-rich atmosphere if it had a global ocean no larger than 0.45 Earth oceans. However, the efficiencies of surface and mantle sequestration processes are very poorly understood for all terrestrial planets (Rosenqvist and Chassefière, 1995). Hamano *et al.* (2013) also suggested that early Venus may have generated a steam atmosphere that slowed planetary cooling and maintained a magma ocean for an extended period after formation; this magma ocean could have also acted as a massive sink for O_2.

On modern-day Venus, the photolytic dissociation rate of CO_2 is high (McElroy *et al.,* 1973), and the atmosphere is largely desiccated, suggesting that the photochemical production of abiotic oxygen or ozone may be possible. Ozone has been detected on the venusian nightside, although with a column abundance 1.5×10^{-4} times less than seen on Earth (Montmessin *et al.,* 2011). Excited O_2—produced by the recombination of O atoms released from CO_2 photolysis—is also detected via its airglow on the venusian nightside. The excited, newly formed O_2 relaxes to the ground state, emitting airglow photons near 1.27 μm (Connes *et al.,* 1979; Allen *et al.,* 1992; Crisp *et al.,* 1996). However, ground-state O_2 has never been detected on Venus, and observational upper limits suggest uniform mixing ratios of <2 ppm above 60 km (Trauger and Lunine, 1983; Mills, 1999). This implies that shortly after its formation, the O_2 is efficiently scrubbed from the atmosphere, possibly by a chlorine-containing catalyst that accelerates the recombination of O with CO to reform CO_2 (Yung and DeMore, 1982). This mechanism has been verified in laboratory experiments (Pernice *et al.,* 2004). Venus' O_3 abundance and spatial distribution also appear to support this mechanism (Montmessin *et al.,* 2011), but the intermediate species have not yet been detected in the venusian atmosphere. Another possible mechanism involves heterogeneous chemistry on aerosols or cloud particles (Mills and Allen, 2007). Little is actually known about these catalytic CO_2 recombination processes; consequently, these mechanisms are not generally included in photochemical codes for terrestrial planets, including the models that were used in the photochemical false-positive studies mentioned above (Hu *et al.,* 2012; Domagal-Goldman *et al.,* 2014; Tian *et al.,* 2014; Gao *et al.,* 2015; Harman *et al.,* 2015). Therefore, determining the sinks for O_2 on Venus is a critical piece of the search for life on exoplanets, as it would place additional constraints on which environments can

accumulate O_2 and allow improvements in photochemical models with regard to O_2/O_3 formation and destruction in terrestrial planet atmospheres. Ultimately, if the mechanisms that drive efficient recombination of CO_2 on Venus also occur on exoplanets, it may make false positives for O_2 more difficult to generate.

4. Implications for the Search for Life beyond Our Solar System

Exploring and understanding the possible mechanisms for abiotic O_2/O_3 production enable identification of planets that are less susceptible to abiotic generation and allow us to recognize planetary and stellar characteristics that will help discriminate between abiotic and biological sources. In the search for life, detecting a candidate biosignature molecule is necessary but not sufficient. To claim a robust detection, environmental abiotic sources for biosignature molecules must also be identified, sought, and excluded. For the first generation of exoplanet characterization missions, spectroscopic observations will be extremely challenging, and biosignatures—and their abiotically generated false positives—will be difficult to detect. Here, we discuss potentially observable characteristics of the planet and planetary system that may allow us to choose the most promising targets for life detection or help identify abiotic sources for O_2 and O_3.

4.1. Target selection considerations

Determining whether a promising planet lies within the star's habitable zone is the first-order assessment performed when selecting planetary targets for spectroscopy. However, in addition to denoting a higher probability for liquid water, the habitable zone could also be used to help screen out those targets that are more likely to exhibit false positives. This latter application will be most effective when conservative habitable zone limits are used (*e.g.,* Kopparapu *et al.,* 2013[1]). Significantly more permissive limits for the habitable zone have been advocated by Seager (2013), for example, for a Sun-like star, an inner limit near the orbit of Mercury [as proposed for low-humidity planets by Zsom *et al.* (2013); see also the discussion by Kasting *et al.* (2014) on the feasibility of these limits] and an outer limit exterior to the orbit of Saturn [as discussed by Pierrehumbert and Gaidos (2011), for H_2-dominated atmospheres]. While these broader limits may include planets with a rare combination of fortuitous characteristics that could support habitability, near their boundaries they are also far more likely to include a higher fraction of planets that could exhibit false positives or false negatives for O_2. At a more permissive inner edge, while some small fraction of terrestrial planets may be habitable, many will be uninhabitable due to higher levels of stellar radiation enhancing Venus-like runaway and water vapor loss processes (Kane *et al.,* 2014). These planets could exhibit abiotic false positives for O_2 or O_3, without requiring an extended higher-luminosity pre-main sequence phase (Schaefer *et al.,* 2016). At a more permissive outer edge, far from the star and with the dense, reducing H_2 atmosphere required to warm the surface, false positives are photochemically unlikely, but false negatives for O_2 may be prevalent, precluding detection of oxygenic photosynthesis, even if present.

While the habitable zone is the first-order means of down-selecting a pool of potentially habitable planetary targets, if there are multiple habitable zone targets, then we will need more comprehensive methods to rank these planets for observation. This ranking could include using observations of the star, planet, and planetary system, along with modeled evolution and environmental constraints to determine the likelihood of both habitability (*e.g.,* Schulze-Makuch *et al.,* 2011; Barnes *et al.,* 2015) and biosignature false-positive generation within the habitable zone. For example, most habitable zone O_2 and O_3 false-positive mechanisms preferentially affect planets orbiting M dwarf stars, which have extended superluminous pre-main sequence phases and UV spectral slopes that are the most favorable for abiotic generation.

Consequently, since these false positives are most likely to affect planets orbiting M dwarfs, they will impact searches for biosignatures using both space-based (Deming and Seager, 2009; Hedelt *et al.,* 2013; Misra *et al.,* 2014b) and ground-based transmission spectroscopy (Snellen *et al.,* 2013; Rodler and López-Morales, 2014), as well as ground-based direct imaging observations, for which Earth-sized planets orbiting M dwarfs are the favored targets (Riaud and Schneider, 2007; Snellen *et al.,* 2015; Crossfield, 2016; Lovis *et al.,* 2016) These smaller, terrestrial planets are easier to detect in transit around lower mass, later-type M dwarfs. This is due to multiple factors [*cf.* Shields *et al.* (2016) for a more detailed discussion], including the more favorable star/planet size ratio, which increases the depth of the transit; the proximity of the habitable zone to the star, which increases the probability of transit; and the concomitant shorter orbital period, which enables more transits to be coadded to increase detectability within a given observing period or telescope lifetime. Later-type M dwarf stars are also favored as likely targets for transmission observations simply because they are the most populous type of star in the local solar neighborhood—with M4V stars (0.2 $M_\odot$, 0.25 $R_\odot$) being the most numerous (Henry *et al.,* 2016)—increasing the likelihood that a nearby planet will be found transiting a member of this population. Indeed, the closest known transiting, and likely terrestrial (with planetary radii $\leq 1.2\ R_\oplus$), exoplanets orbit GJ 1132, an M3.5V star (Berta-Thompson *et al.,* 2015) and TRAPPIST-1, an M8V star (Gillon *et al.,* 2016, 2017).

4.1.1. Target selection for transmission.

The existing studies suggest that false positives for O_2 and O_3 in transit spectroscopy can be mitigated by selecting planets in the habitable zones of earlier-type M dwarfs—although this is clearly at odds with the other target selection criteria described above. To avoid those planets most susceptible to generating large amounts of false O_2, the work of Luger and Barnes (2015, their Fig. 13) suggests that we should target planets orbiting stars more massive than 0.4 $M_\odot$ (M3V and earlier) and especially favor those planets found toward the outer edge of the habitable zone around these stars. These earlier-type, brighter stars would backlight a planet's atmosphere more strongly and so would produce stronger signals than later-type M dwarfs at a given distance from the observer. However, there may be fewer of these targets available, as these earlier-type M dwarfs are less common, and their habitable zone planets, which orbit farther from their

[1]http://depts.washington.edu/naivpl/sites/default/files/hz.shtml

star, would be less likely to be found in transit. Clearly, the selection of targets in the habitable zone for transmission spectroscopy will not be straightforward and will need to be made on a case-by-case basis. It will depend on the number of suitable targets available, the brightness of the host star and other observability considerations, the likelihood that the planet is habitable (*e.g.,* Barnes *et al.,* 2015), and the probability that the planet and star combination is susceptible to the abiotic generation of biosignatures such as O_2 and O_3.

4.1.2. Target selection for direct imaging. For direct imaging considerations, target selection to avoid the likelihood of abiotic O_2 or O_3 generation depends primarily on whether the planets are to be imaged with ground-based or space-based telescopes. Future large (30–40 m diameter) ground-based telescopes planned for 2020 and beyond (*e.g.,* Quanz *et al.,* 2015) will have the capability to directly image about 5–10 terrestrial planets orbiting in the habitable zones of nearby bright M dwarfs (Crossfield, 2016). Space-based telescopes for direct imaging—anticipated to launch on the 2020–2040 timeframe—will necessarily have smaller mirror diameters and will find it more challenging to observe M dwarf habitable zone planets, instead focusing primarily on F, G, and K dwarfs (Stark *et al.,* 2014).

For ground-based telescopes, the focus on directly imaging M dwarf habitable zone planets means that these telescopes will encounter similar target selection issues as transmission observations, namely prioritizing earlier-type M dwarfs and avoiding late-type M dwarfs as planet hosts, or at least considering these targets with caution. Although M dwarf habitable zones are much closer to the star—and so have a relatively small angular separation between star and planet—the large diameter of future ground-based telescopes (30–40 m) will provide adequate angular resolution to observe nearby M dwarf systems in the visible and NIR (*e.g.,* Kawahara *et al.,* 2012; Snellen *et al.,* 2015). It may even be possible to observe Proxima Centauri b out to 0.78 μm by upgrading instrumentation on the existing 8.2 m diameter Very Large Telescope (Lovis *et al.,* 2016). The main advantage M dwarf habitable zone planets provide for ground-based direct imaging is that these planets will have the most favorable contrast between planet and star at NIR and IR wavelengths, where the use of adaptive optics to remove the effects of turbulence in Earth's atmosphere has the best performance (Males *et al.,* 2014; Snellen *et al.,* 2015).

Spaceborne direct imaging missions such as the Wide Field InfrarRed Survey Telescope (WFIRST; Spergel *et al.,* 2015) and mission concepts currently being considered for a High Definition Space Telescope (HDST; Dalcanton *et al.,* 2015) such as the Habitable Exoplanet Imaging Mission (HabEx; Mennesson *et al.,* 2016) and the Large Ultraviolet Optical Infrared Survey Telescope (LUVOIR; Bolcar *et al.,* 2015) will complement transmission spectroscopy and ground-based direct imaging by focusing primarily on planets orbiting F, G, and K dwarfs (Dalcanton *et al.,* 2015), with M dwarfs being less than 10% of their anticipated targets (Stark *et al.,* 2014, 2015). Even the most ambitious space-based direct imaging missions will have smaller mirror diameters than their ground-based counterparts, making it challenging to separate habitable zone planets from their late-type M dwarf (*e.g.,* M3V and later) hosts, even for very nearby targets (*e.g.,* Meadows *et al.,* 2016). Consequently, the bulk of their survey samples will consist of planets that will be less susceptible to many of the known false-positive mechanisms that affect later-type M dwarfs. However, F dwarf planets may still be affected by high levels of abiotic O_3 generation from CO_2 photolysis (Domagal-Goldman *et al.,* 2014), and planets orbiting F-K dwarfs may also be susceptible to abiotic O_2 generation if their atmospheres have a lower abundance of noncondensable gases (Wordsworth and Pierrehumbert, 2014). The degree to which a planet has an atmosphere rich in CO_2, or a noncondensable atmospheric component, is dependent primarily on planetary and planetary system properties, including planet formation and evolution, and the delivery of volatiles from the protoplanetary disk. Planetary atmospheres that favor abiotic O_2 or O_3 generation are therefore a fundamental planetary property and largely independent of the characteristics of the host star, which are more readily observable. In the absence of information about the planet's atmosphere, it will be difficult to identify in advance planets susceptible to these mechanisms of abiotic O_2 or O_3 generation. Target selection considerations for space-based direct imaging will therefore focus more practically on the suite of planetary and stellar characteristics that increase the likelihood of planetary habitability. Indications that O_2 or O_3 is being abiotically generated will come from spectroscopic observations of the planetary environment.

4.2. Recognizing abiotic O_2 and O_3

Consequently, since target selection can mitigate, but not preclude, the possibility of false positives in transit and direct imaging observations, it will be important to also understand which measurements will help directly identify an increased likelihood of abiotic generation of O_2 or O_3. These measurements can either be made via transit transmission or secondary eclipse, especially for M dwarfs (*e.g.,* Rauer *et al.,* 2011; Arnold *et al.,* 2014), or via direct imaging for all spectral types (*e.g.,* Meadows *et al.,* 2016; Schwieterman *et al.,* 2016a,b). For ground-based telescopes, additional techniques must be used to mitigate the effect of absorption in Earth's atmosphere, which contains similar molecules to those being sought in terrestrial exoplanet atmospheres. These techniques include the use of high-resolution spectroscopy ($R \sim 100{,}000$) to observe spectral features that shift in wavelength with the radial component of the orbital motion of the exoplanet. This behavior can then be used to separate the planet's absorption from the relatively stationary telluric and stellar lines (Snellen, 2014). This technique can be used for ground-based observations of transmission spectra from exoplanets (*e.g.,* Snellen *et al.,* 2013; Rodler and López-Morales, 2014), although many transits will need to be coadded to obtain enough signal on the planet. With the planet only available at favorable geometries for $\sim$10 h per year, the entire observation could take several to 10 years to complete (Crossfield, 2016; Lovis *et al.,* 2016). Recently, several research groups have explored combining ground-based high-angular-resolution direct imaging—including starlight suppression—with high-spectral-resolution spectroscopy to further suppress light from the star and observe molecules in the exoplanet atmosphere (Kawahara *et al.,* 2012; Snellen *et al.,* 2015; Lovis *et al.,* 2016). Brogi *et al.* (2016) have also pioneered a technique that combines low-resolution

spacecraft observations of a given exoplanet target with high-resolution ground-based observations to enhance the information retrieved from both data sets, allowing retrieval of molecular abundances from the spectra.

Habitable zone planets orbiting M dwarfs have several intrinsic advantages for characterization via transmission, compared to planets orbiting other stellar types. They are less affected by refraction in the planetary atmosphere, and the favorable star/planet size ratio produces deeper spectral features for atmospheric gases. Refraction can limit how deep into an aerosol-free planetary atmosphere a transmission spectrum can probe, precluding sampling below ~13 km in the planetary atmosphere for an Earth-Sun analogue (García Muñoz *et al.,* 2012; Bétrémieux and Kaltenegger, 2013, 2014; Misra *et al.,* 2014b). However, due to a more favorable geometry, refraction is not the limiting factor in probing deeper altitudes for planets orbiting later-type M dwarfs, and accessing the lowest atmospheric layer is theoretically possible (Bétrémieux and Kaltenegger, 2014; Misra *et al.,* 2014b). However, in practice, the wavelength-dependent opacity of a terrestrial planetary atmosphere will limit how deep in the atmosphere a transmission spectrum is able to probe. This opacity will be a function of the atmosphere's composition and mass, and includes the effects of Rayleigh scattering. A minimum altitude of 5 km above the surface near 1 μm has been simulated for modern-Earth-twin planets orbiting M dwarfs of M5V and later (*e.g.,* Bétrémieux and Kaltenegger, 2014). However, simulated transmission spectra for planets with different atmospheric compositions orbiting M dwarfs, including CO_2-dominated planets, and photochemically self-consistent Earth-like and early Earth-like planets (with higher CH_4 and CO_2 fractions than modern Earth), show minimum altitudes closer to 10 km and above near 1 μm (Meadows *et al.,* 2016; Arney *et al.,* 2017). A 10 km altitude is within the troposphere for an Earth-like planet but well above the majority of tropospheric water vapor, and Earth's clouds. This is important for biosignature detection and false-positive assessment, as the planet's troposphere usually contains a significant fraction of the atmospheric mass (80% in the case of Earth), and the near-surface environment is most likely to record the presence of surface and interior processes such as life, volcanism, and a hydrological cycle.

Direct imaging observations measure reflected or emitted light from the planet, and this method is potentially useful for studies of planets orbiting all stellar types, as long as the star and habitable zone planet can be angularly resolved, either by using a large-enough mirror diameter (*e.g.,* Snellen, 2014; Stark *et al.,* 2015) or by improving how close to the star its light can be suppressed to a sufficient level for the planet to be observed (the ''inner working angle,'' or IWA). The IWA can be improved with various starlight suppression techniques including coronagraphy for ground- and space-based telescopes (*e.g.,* Beuzit *et al.,* 2008; Stapelfeldt *et al.,* 2015; Robinson *et al.,* 2016) or the use of a starshade spacecraft that flies in front of a space telescope to block light from the host star (Cash, 2006; Seager *et al.,* 2015). Direct imaging observations can be used to obtain a disk-averaged photometric or spectroscopic measurement that captures light from the top of the planetary atmosphere down to the emitting or reflecting layer—which could be a haze, cloud, a level of the atmosphere, or the actual planetary surface. Because the path taken by the direct imaging observation through the atmosphere is more direct than the limb-skimming path of a transmission observation, direct imaging observations complement transmission observations because they can see much deeper into a planetary atmosphere, and possibly all the way to the surface—and are less sensitive to the attenuating effects of hazes and other upper atmospheric absorbers (Arney *et al.,* 2016). Below we discuss how these two techniques—transit transmission and direct imaging—could be used to help discriminate between abiotic and biological sources of O_2.

4.2.1. Discriminating the effects of enhanced pre-main sequence stellar luminosity. The buildup of thousands of bar of O_2 due to catastrophic loss of water vapor during an M dwarf's pre-main sequence phase is the strongest false positive for O_2 currently suggested (Luger and Barnes, 2015; Tian, 2015). Identifying the presence of a massive, and therefore likely abiotic, oxygen atmosphere could be done by detecting absorption from O_2 collisional pairs (O_4) in the spectrum of the planet for both transmission and direct imaging observations (Schwieterman *et al.,* 2016a, 2016b). In contrast to O_2 absorption, which is directly proportional to the number density of the gas, the collisionally induced absorption of O_4 has a density-squared dependence, so it increases in strength—relative to O_2—as the number density of the gas increases (*e.g.,* Misra *et al.,* 2014a). In transit transmission, for modest atmospheric pressures (up to 10 bar) and O_2 fractions (<20%), O_4 features are potentially detectable—although extremely challenging—near 1.06 and 1.27 μm (Misra *et al.,* 2014a). However, for O_2-dominated atmospheres of at least a bar, simulated spectra of self-consistent climate-photochemistry models show significantly stronger NIR features at 1.06 and 1.27 μm in transmission spectra, but the O_4 features shortward of 1.06 μm are not detectable due to the masking effects of Rayleigh scattering induced by the long transmission path lengths through these dense atmospheres (Fig. 2a; Schwieterman *et al.,* 2016a). Consequently, a wavelength range of at least 0.6–1.3 μm would be needed to search for O_4 and thereby identify likely abiotic O_2 in transmission observations. Interestingly, Schwieterman *et al.* (2016a) showed that for an example 100 bar O_2 atmosphere (equivalent to the loss of 40% of an Earth ocean) the NIR O_4 features are stronger and more detectable than the O_2 features in transmission spectra. In this case, the discriminator of the abiotic source of the O_2 would be detected in transmission spectra *before* the false positive itself. Once the telltale O_4 was detected, the decision could be made to either continue the observations or move on to a more promising target.

For direct imaging spectra, O_4 features in both the visible and NIR could be detected. The O_4 features can be stronger for direct imaging for the same atmospheric composition when compared to transmission, as the shorter-pathlength, downward-looking observations probe deeper, denser regions of the atmosphere where the density-dependent O_4 molecules are more likely to form. This shorter pathlength also reduces masking by Rayleigh scattering, and even at 1 bar of O_2 the corresponding O_4 features in the visible from 0.34 to 0.65 μm become significant (see Fig. 1 in Schwieterman *et al.,* 2016b)—in addition to the NIR features at 1.06 and 1.27 μm. Consequently, observations at 0.4–1.0 μm may be all that is needed to search for O_4 to discriminate

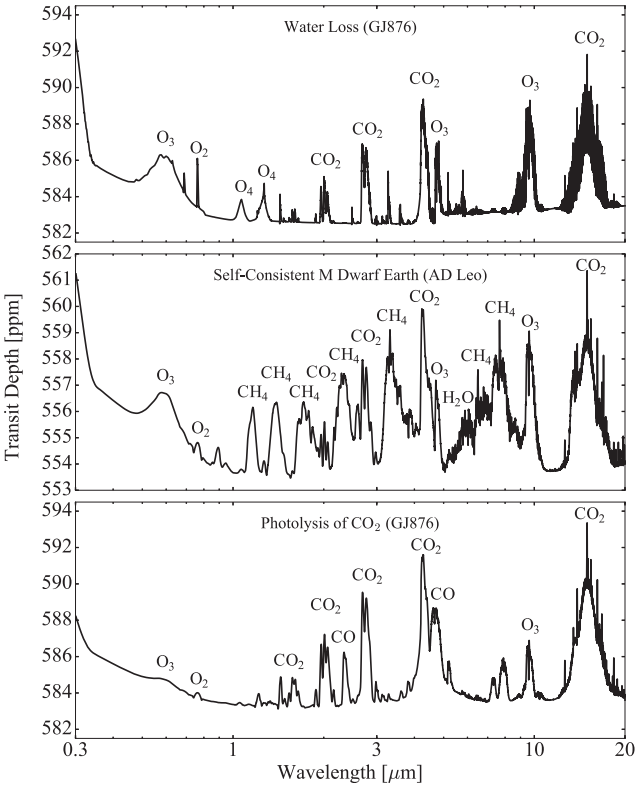

FIG. 2. Transmission spectra of three simulated terrestrial planets orbiting M dwarfs. (Top) The transmission spectrum of a 1 bar, 95% O_2 atmosphere generated by loss of water from a pre-main sequence M dwarf (Luger and Barnes, 2015; Schwieterman *et al.,* 2016a,b). Although the abiotic O_2 absorption at 0.76 μm is quite strong, the much stronger collisionally induced O_4 bands in the planet's spectrum would indicate the presence of a more massive O_2 atmosphere. (Middle) For comparison, the transmission spectrum of a planet with Earth-like surface fluxes, including O_2 fluxes from photosynthesis, that has photochemically and climatically interacted with the spectrum of its parent star. Note the prevalence of not only O_2 and O_3 but strong CH_4 as well. (Bottom) The transmission spectrum of a planet with abiotic O_2 at an abundance of 6%, generated by photolysis of CO_2 (Harman *et al.,* 2015; Schwieterman *et al.,* 2016a,b). The O_2 is weak and unlikely to be detectable; however, both CO and CO_2 are prominent in this spectrum and would serve as beacons to indicate that the O_2 observed may be due to CO_2 photolysis. (Credit: J. Lustig-Yaeger, E. Schwieterman)

abiotic O_2 in direct imaging observations. These visible wavelength O_4 features are well within the wavelength range proposed for NASA direct imaging mission concepts such as WFIRST (Spergel *et al.,* 2015), Exo-C/S (Seager *et al.,* 2015; Stapelfeldt *et al.,* 2015), and the HabEx/LUVOIR concepts in support of a HDST (Dalcanton *et al.,* 2015) and can be taken simultaneously or near-simultaneously with the O_2 measurement itself. However, as discussed, M dwarf habitable zones are challenging to observe with direct imaging, and the first generation of direct imagers (*e.g.,* WFIRST) will struggle to spectrally characterize habitable zone super-Earths. The best targets will also be orbiting hotter F and G dwarf stars, where catastrophic loss of H_2O in the main sequence habitable zone, and the corresponding O_2 false positive, is less likely. In these cases, massive O_2 atmospheres may only be seen for close-in planets with significantly higher insolation levels than Earth. It is also important to note that O_4 collisionally induced absorption is a broad continuum absorption, and high-resolution ground-based spectroscopy will find it extremely challenging to separate the planet's O_4 absorption from that in Earth's atmosphere.

It is important to stress that obtaining near-term spectra of ''hot Earths'' or ''exo-Venuses''—terrestrial exoplanets that orbit closer to the star than the currently defined habitable zone limits—will support our future interpretation of O_2 as a biosignature by providing a crucial observational test of the evolution of terrestrial planet atmospheres (Schaefer *et al.,* 2016) and the proposed ocean-loss false-positive mechanism (Luger and Barnes, 2015). Hot Earths orbiting M dwarfs would have too high an insolation level to be habitable, and the detection of O_2 or O_4 in these atmospheres would confirm the efficacy and longevity of this potential false positive. Conversely, if more desiccated, CO_2-rich, O_2-poor Venus-like atmospheres are detected, especially for older stars, this may indicate that close-in terrestrial planets are able to effectively lose, or internally sequester, O_2 from a lost ocean (*e.g.,* Schaefer *et al.,* 2016), or that these planets form dry. Even in advance of the first direct imagers, JWST transmission spectra or ground-based observations of the atmosphere of transiting ''super-Venus'' M dwarf planets may prove interesting as potential tests of this abiotic O_2 mechanism, and indeed of the calculated limits of the habitable zone itself. A potential candidate for these observational tests includes GJ 1132b (Berta-Thompson *et al.,* 2015) which receives 19 times Earth's insolation ($\sim$3 times Mercury's insolation) and orbits an M3.5V, at least 5-billion-year-old star. Similarly, the recently discovered TRAPPIST-1b and TRAPPIST-1c planets (Gillon *et al.,* 2016, 2017), which orbit an M8V dwarf believed to be older than 500 million years, both receive insolation in excess of Venus', at 4.3 and 2.3 times Earth's insolation, and would have likely experienced an extended pre-main sequence superluminous phase from their parent star (Baraffe *et al.,* 1998).

4.2.2. Discriminating the effects of low noncondensable gas inventories. Observations that set limits on a terrestrial exoplanet's noncondensable gas abundances—and in particular the O_2/N_2 ratio in the planetary atmosphere—could be used to identify the likely generation of abiotic O_2 via weak cold-trapping of water vapor in atmospheres with small noncondensable gas inventories. Although the O_2 is formed from water photolysis, these atmospheres will not necessarily be depleted in water vapor, so detection of water vapor would not conclusively rule out abiotic O_2 production in this case. Rayleigh scattering could be used to attempt to determine overall atmospheric pressure and therefore deduce an ''invisible'' component that may be N_2 or another gas that is otherwise not spectrally active in the observed wavelength range. For an Earth-like planet seen in direct imaging, the observed Rayleigh scattering will be influenced by the different atmospheric columns probed over clear sky and cloudy scenes, returning a disk-averaged value for atmospheric pressure that will be systematically lower than the actual surface pressure. Additionally, this technique for pressure determination can be highly inaccurate in the presence of planetwide clouds and hazes that limit the

observable atmospheric column. This is the case for Venus, where high sulfuric acid hazes truncate the observable atmosphere at 30 mbar at visible wavelengths. This technique will also have low accuracy if Rayleigh scattering is countered or masked by a blue absorbing component on the planetary surface or in its atmosphere, as would be the case for iron oxides in the martian surface or hydrocarbon hazes on an early Earth (Arney *et al.,* 2016). However, all of these mechanisms tend to reduce the observed Rayleigh scattering effect, so if a strong Rayleigh scattering slope is still observed, it may be a good indicator of higher atmospheric pressure and a subsequently lower likelihood of a lower noncondensable gas fraction. Similarly, pressure-dependent effects, such as the presence of collisionally induced absorption of any kind (Richard *et al.,* 2012), condensates, or broad molecular absorption bands, may also point to more massive atmospheres and could possibly be used to rule out a lower-pressure atmosphere. It has also been suggested that an averaged N_2 column density might be determined from measurements of O_2-N_2 collisionally induced absorption near 1.27 μm along with other O_2 bands (Pallé *et al.,* 2009). However, it may prove challenging to disentangle the effects of the O_2-N_2 absorption from O_4 and O_2 absorption and emission, which also occurs near 1.27 μm.

The most unambiguous discriminant, but potentially the most challenging to observe, would be detection and quantification of pressure-dependent O_4 and N_4 collisionally induced absorption. Determination of the oxygen partial pressure for a terrestrial planet may be achieved by observing O_2 collisional pairs in either transmission—challenging for JWST (Misra *et al.,* 2014a)—or direct imaging, as discussed above. For N_2, absorption from collisional pairs (N_4) could be sought near 4.1 μm. This absorption is broader at high abundance and could help constrain N_2 fraction (Schwieterman *et al.,* 2015b). Consequently, to discriminate this abiotic O_2 generation mechanism with the least ambiguity, observations of O_2 and N_2 collisional pairs, over a wavelength range from 0.6 to 4.5 μm for transmission and 0.4 to 4.5 μm for direct imaging, would be desirable. These longer wavelengths may be accessible, but challenging, for transmission, although transmission cannot probe to the planet's surface, making the resulting pressures difficult to interpret. For space-based direct imaging telescopes, for which planets orbiting F, G, and K stars will be the majority of the targets, telescope mirror diameter and temperature would likely mean that only a handful of habitable zone planets would be observable at the longer wavelengths needed to detect N_4. Ground-based high-spectral-resolution observations may also struggle to observe the broad continuum of the N_4 collisionally induced absorption and separate it from Earth's. These challenges suggest that alternative means for discriminating this false positive should also be explored and identified.

4.2.3. Discriminating the effects of CO_2 photolysis in a desiccated atmosphere. M dwarf planets may also produce another significant false positive for O_2—for the high CO_2, low H inventory atmospheres that do not catalyze CO_2 recombination. These atmospheres may produce stable O_2 abundances of 10–15% for total hydrogen mixing ratios less than 1 ppm (Gao *et al.,* 2015). However, in this mechanism, both CO_2 and CO would constitute large fractions of the atmosphere and would be more detectable in transit spectra than the abiotic O_2 (Schwieterman *et al.,* 2016a), requiring a wavelength range of 0.6–2.5 μm in transmission to discriminate. For direct imaging, CO_2 and CO may also be present but are likely to be more challenging to observe than in transmission, due to weaker signals in the shorter pathlengths of direct imaging (Fig. 3b; Schwieterman *et al.,* 2016a, 2016b; Wang *et al.,* 2016). However, the extreme desiccation required for this mechanism to work would manifest as little or no water vapor absorption at either reflected visible to NIR or emitted MIR wavelengths (Gao *et al.,* 2015), and strong O_2 without corresponding water absorption bands in direct imaging could be used to discriminate this process (over a wavelength range of only 0.6–1.0 μm). For ground-based high-resolution spectroscopy, observations in the visible and NIR of O_2, CO_2, CO, and an unsuccessful search for H_2O in either transmission or direct imaging, may help discriminate this false positive.

4.2.4. Discriminating the effects of CO_2 photolysis in a habitable atmosphere. Finally, for N_2- and H_2O-rich habitable zone planets, abiotic generation of O_2 or O_3 by photolysis is still possible, but in these cases the models predict

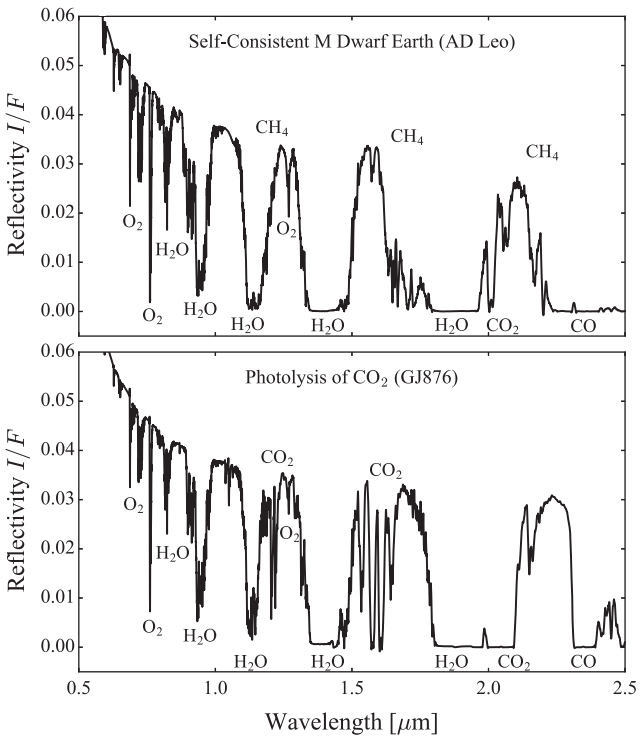

FIG. 3. Simulated reflectivity spectra of CO_2 photolysis atmospheres and a self-consistent M dwarf Earth. (Top) The reflectivity spectrum for the planet in Fig. 2 with Earth-like surface fluxes, that has photochemically and climatically interacted with the spectral energy distribution of its parent M3.5V dwarf star. (Bottom) Reflectivity spectrum for the CO_2-rich planetary atmosphere with 6% abiotic O_2 plotted in transmission in Fig. 2. This comparison shows that the presence of CH_4 for the Earth-like planet and the strong absorption from CO_2 and CO for the planet orbiting GJ 876 can be used to discriminate between the biological and abiotic source of the O_2 seen in these spectra. (Credit J. Lustig-Yaeger, E. Schwieterman)

relatively small amounts, and for the O_2 in particular, these will be extremely challenging to detect with next-generation telescopes. In Domagal-Goldman *et al.* (2014), the highest abiotic O_3 produced, 0.1 PAL, occurred for planets orbiting stars with relatively high FUV fluxes, such as F dwarfs. This abiotic abundance can produce a Hartley O_3 absorption band (0.2–0.3 μm) that is comparable to that of modern Earth. However, the lower, 0.1 PAL O_3 abundance from this abiotic mechanism becomes apparent when looking at other O_3 features in the visible—which are much weaker than Earth's—and could be used to help to quantify the total O_3 column abundance (Domagal-Goldman *et al.,* 2014). The high-FUV M3.5 dwarf AD Leo also produced a relatively large absorption feature at UV wavelengths but with negligible O_2 or O_3 absorption features elsewhere in the spectrum. In this case then, the false positive is confined to observations at UV wavelengths, which will not be observable for habitable zone exoplanets with JWST, WFIRST, or ground-based extremely large telescopes and must wait for HDST-class telescopes in the 2030+ time frame.

Domagal-Goldman *et al.* (2014) also showed that generally, production of abiotic O_3 by CO_2 photolysis only occurred in atmospheres with high CO_2 concentrations and low CH_4 concentrations. The CO_2-rich atmospheres required could produce multiple strong CO_2 features between 1 and 2 μm, which could be sought as discriminants. Observation of strong CH_4 could also be used as a proxy for the reducing power of the atmosphere, as high CH_4 abundances make abiotic production of O_3 far less likely. However, quantifying the CH_4 abundance to help determine the redox state of the atmosphere will likely be challenging for direct imaging observations of M dwarf planets in the UV-visible-NIR, as the strongest CH_4 features are in the NIR. Due to the wavelength dependence of the IWA constraint—that angular distance from the star where its light is first suppressed sufficiently to measure the planet—these longer wavelengths may not be accessible for all but the closest M dwarf planetary systems, due to the small angular separation of the M dwarf star and its habitable zone planet. However, Lovis *et al.* (2016) suggested that a search for O_2, H_2O, and CH_4 could be performed for Proxima Cen b using coupled high-resolution imaging and spectroscopy on ground-based telescopes over the 0.6–0.78 μm visible range.

In Tian *et al.* (2014) and Harman *et al.* (2015), the models and boundary conditions generated more abiotic O_2 than seen in Domagal-Goldman *et al.* (2014). However, with reasonable sinks included, the amount of O_2 generated was still extremely small when compared to modern-day Earth values. In addition, abiotic O_2 buildup was again most abundant for planets orbiting M dwarfs, which will be difficult to observe with direct imaging. Tian *et al.* (2014) did not generate spectra of their model atmospheres, and their detectability arguments for the 0.2% abiotic O_2 (a hundredth of Earth's current O_2 abundance) were made by comparing to previously generated synthetic spectra for similar O_2 and O_3 abundances, from Segura *et al.* (2003). Since the abundance of O_3 generated from O_2 is extremely nonlinear (Kasting and Donahue, 1980), a factor of 100 drop in O_2 abundance can result in only a 60% reduction in the ozone column depth for a planet orbiting a Sun-like star (Segura *et al.,* 2003). O_2 absorption, however, does drop in much closer correspondence to the abundance drop, and the equivalent width of the O_2 0.76 μm A-band for 0.2% O_2 will be only 1% of that of modern-day Earth's. This will likely not be detectable by the first or even second generation of terrestrial exoplanet direct imaging missions (WFIRST and HDST-class), even if there is an accessible M dwarf planetary candidate. JWST would be more likely to observe such a planet, and JWST transit spectra will require several hundred hours to observe present-day Earth's abundance of O_2 in a terrestrial planet atmosphere (Fig. 4; Cowan *et al.,* 2015; Schwieterman *et al.,* 2016a), so observing a signal that is 100 times weaker will be infeasible during the mission lifetime.

Similarly, the O_2 false positive defined by Harman *et al.* (2015) as anything in excess of the Planavsky *et al.* (2014b) estimate of Proterozoic O_2, namely 10^{-3} PAL, is highly unlikely to be detectable by near-future telescopes operating in the visible. The resultant O_3 features in the UV and MIR will be stronger, but in the MIR, detection of O_3 at 9.6 μm can be complicated by abundant atmospheric CO_2, which produces strong and broad 9.4 μm absorption from CO_2 hot bands (Selsis *et al.,* 2002). Observations at these wavelengths in transmission will also be even more challenging due to the strong falloff of the host star's blackbody at these longer wavelengths. The highest abiotic O_2 abundance of 6% for a planet orbiting GJ 876 assumed no sinks for O_2 in the planetary atmosphere, and this amount dropped by a factor of 1000 when more realistic boundary conditions were used (Harman *et al.,* 2015). Six percent O_2 may be detectable by future larger-aperture direct imaging telescopes on the ground or in space, for a nearby M dwarf with an accessible habitable zone (*i.e.,* at a larger angular separation than the IWA). However, this amount will still be extremely challenging for JWST to detect. Even with 6% O_2, the signal is at the 1 ppm level in the simulated JWST transmission spectrum (Fig. 2), which is likely not achievable. Also, as was the case for the desiccated CO_2 atmospheres, in both the Harman *et al.* (2015) and Tian *et al.* (2014) atmospheres, the abundant CO_2, and CO—the photolytic by-product of abiotic O_2 production—would be more readily detectable than the false O_2 signal itself (Fig. 2), alerting observers to the likely abiotic origin for the O_2 (see Schwieterman *et al.,* 2016a, their Fig. 2). Consequently, it is highly unlikely that the photochemical methods of abiotic O_2/O_3 generation are going to significantly impact observations made with JWST or HDST (HabEx/LUVOIR). Ground-based observations would also have the option to search for CO as well as O_2 in the spectrum (Snellen, 2014), which could help discriminate this false positive.

However, although JWST is unlikely to detect abiotically generated O_2 from CO_2 photolysis, it is generally true that transmission observations are more sensitive than direct imaging to photochemically generated O_2 or O_3. Abiotic O_2 generation from the photochemical destruction of CO_2 and H_2O is most effective in the stratosphere, where UV photons are not attenuated and where geometry and relative atmospheric transparency maximize the transmission signal for trace gases. And while production occurs high in the atmosphere, sinks for O_2 or O_3 from either volcanic outgassing of reduced gases or reactions in seawater are concentrated in the near-surface troposphere, resulting in a profile where abiotically generated O_2 may be less abundant near the surface (see, *e.g.,* Harman *et al.,* 2015, their Fig. 8).

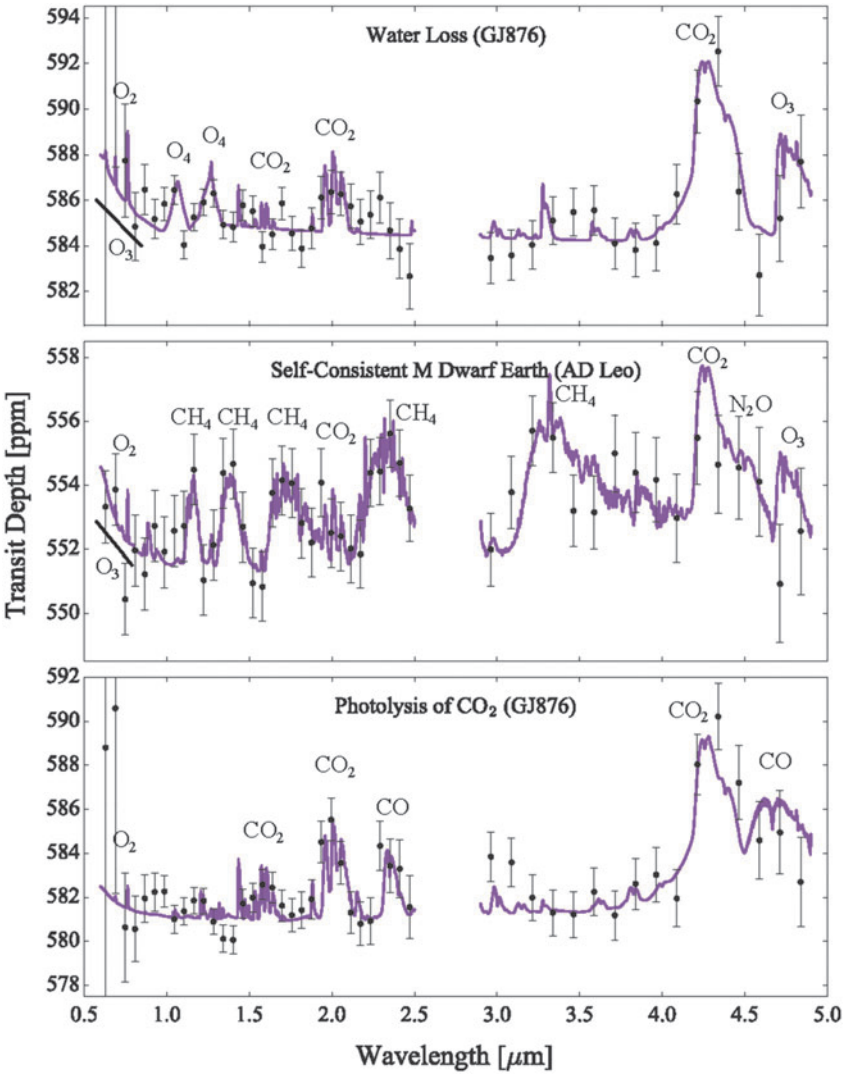

FIG. 4. Simulated JWST observations of the three simulated planets from Fig. 2. Synthetic JWST/NIRISS and JWST/NIRSPEC observations (simulations performed by Drake Deming; Schwieterman *et al.,* 2016a,b) of an O_2-rich water loss atmosphere (Top), a self-consistent M dwarf Earth (Middle), and the CO_2-rich atmosphere (Bottom). These results are for 10 transits, corresponding to about 65 h of JWST time for each object and instrument. The observed points are in black, and to improve the S/N the wavelength resolution has been degraded by coadding the 2048 resolution elements of the detector down to 32 columns. Photon-limited noise was used in the simulations, assuming on-orbit instrument performance and exoplanet-tailored observing techniques will ultimately be able to achieve this. The intensity of the star backlighting the planet's atmosphere begins to drop at longer wavelengths, so the photon-limited S/N will decrease, resulting in larger error bars. Note that the features seen here with the assumed photon-limited noise are of the order of 2–8 ppm, which is below the instrument systematic errors assumed prelaunch (Greene *et al.,* 2016). These observations will therefore be extremely challenging and will depend ultimately on on-orbit performance of the JWST science instruments and excellent knowledge of instrument systematics and how to ameliorate them. (Credit: J. Lustig-Yaeger, D. Deming, E. Schwieterman)

In contrast, biological O_2 fluxes are likely concentrated near the surface, resulting in higher near-surface abundances, or if the O_2 is abundant, an O_2 profile that is evenly mixed throughout the atmospheric column.

Looking to the future, larger-aperture, more sensitive telescopes may be able to measure this altitude-dependent disparity in abiotic O_2 abundance, if they are able to take sensitive, time-dependent observations of a planet as it transits. This may be possible using the effects of refraction on observations of transiting planets, as prior to ingress (and post egress), when the planet is not yet on the stellar disk, refracted light can probe deep into a planet's atmosphere, whereas observations of the planet on the star's disk probe higher in the atmosphere (Misra *et al.,* 2014b). These observations would require relatively short exposures to yield sufficient temporal resolution that different levels of the planetary atmosphere can be probed during the ingress and egress phases. An advanced telescope—well beyond JWST's capabilities—would be needed to make such a measurement. This could be a possible complementary technique for HDST-class or ground-based extremely large telescopes that are built for direct imaging of exoplanets but still have the aperture size to make sensitive transmission measurements, if a suitable target is available.

5. Synthesis and Future Work

In summary, recent research has improved our understanding of potential false positives for O_2 and shown that each false-positive mechanism may reveal itself via observable properties of the planet or star. The recently identified abiotic sources of large atmospheric fractions (>6%) of O_2 for habitable zone planets are as follows: early stellar evolution and planetary atmospheric hydrogen loss (Luger and Barnes, 2015; Tian, 2015), lack of noncondensable species (Wordsworth and Pierrehumbert, 2014), photochemical production in atmospheres with no aqueous CO sinks (Harman *et al.,* 2015), and desiccated, CO_2-dominated atmospheres (Gao *et al.,* 2015). These mechanisms all have additional environmental and spectroscopic features that would help distinguish an abiotic source from a photosynthetic biosphere, whether that be stellar UV spectrum, atmospheric composition, or the presence of liquid water (Fig. 5).

However, these discriminants have varying degrees of observability relative to the false O_2 signal itself. Observation of collisional pairs of O_2 molecules, O_4, could discriminate O_2 generated by atmospheric loss, and the O_4 molecule may be more detectable than the O_2 molecule in both direct imaging and transit spectra (Misra *et al.,* 2014a;

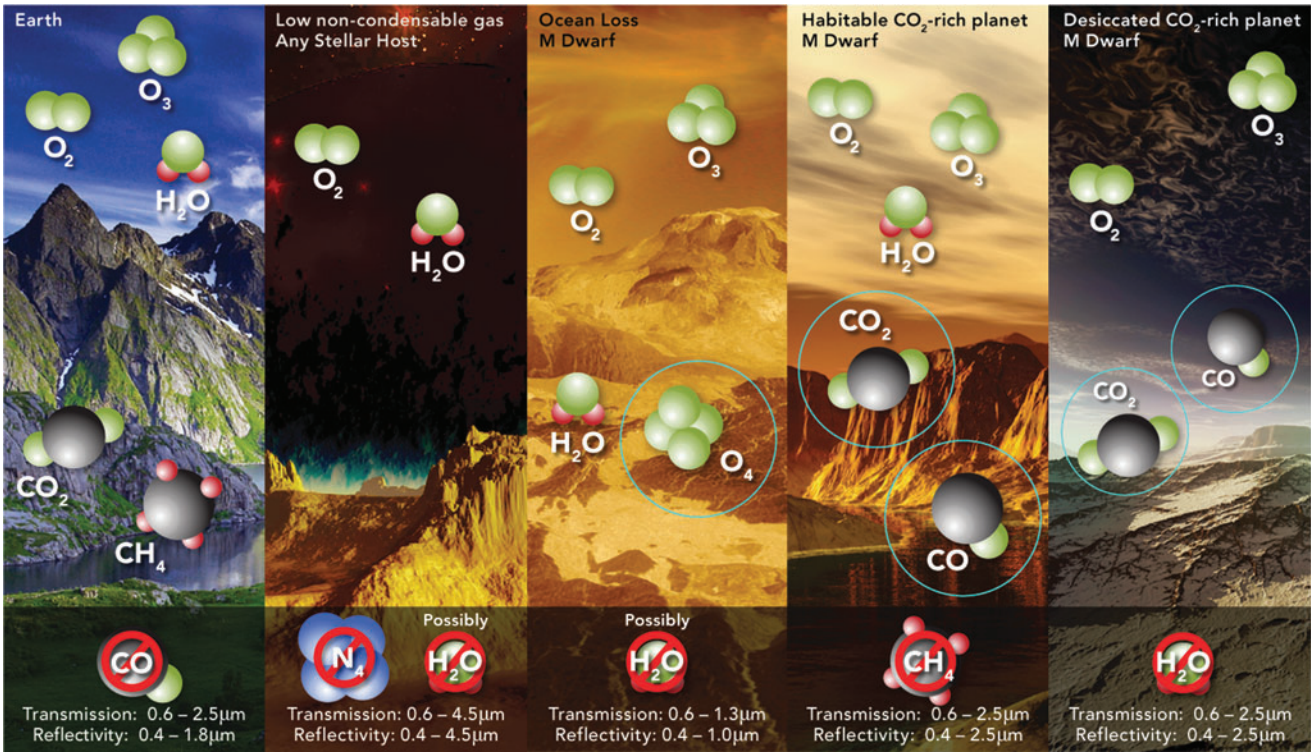

FIG. 5. Discriminating false positives for different environments. For a photosynthetic biosphere (Left) the simultaneous presence of O_2, O_3, CH_4, and the absence of a large abundance of CO points to a photosynthetic origin for Earth's O_2. In the remaining panels, we show the predominant molecules for various false-positive scenarios, the molecular discriminants whose presence indicates a false-positive mechanism (circled), and the missing molecules (in the bottom region) whose absence indicates a likely false-positive mechanism. The nominal wavelength ranges needed to observe these discriminants or check for their absence are given at the bottom of each panel. From left to right (after Earth), abiotic O_2 from water photolysis due to a low noncondensable gas inventory; a massive O_2 atmosphere from water loss in which H_2O may or may not still be present; a habitable world—in which a combination of M dwarf stellar spectrum and reduced atmospheric and surface sinks for O_2 has resulted in the buildup of abiotic O_2 from CO_2 photolysis, or the generation of abiotic O_3; and a desiccated, H-poor environment in which O_2 is a stable photolytic by-product of CO_2. (Credit R. Hasler, V. Meadows, S. Domagal-Goldman)

Schwieterman *et al.,* 2016a, 2016b). The presence of strong CO and CO_2 in transmission spectra would also point to an abiotic origin from CO_2 photolysis for observed O_2 (Wang *et al.,* 2016) and would also likely be more detectable than the O_2 itself (Schwieterman *et al.,* 2016a,b). Determining the abundance of noncondensable species in a planetary atmosphere will be far more difficult, however, as atmospheric pressure measurements for terrestrial planets are challenging and in the presence of clouds can be difficult to interpret. While searching for N_2 in the planet's spectrum is desirable, at non-UV wavelengths N_2 is only accessible through its collisional pair at 4.1 μm, and this is a challenging observation to make (Schwieterman *et al.,* 2015b). Consequently, more work is needed to find alternative ways to identify a low noncondensable gas atmosphere.

Other proposed mechanisms that rely on the UV spectrum of the star to preferentially build up abiotic O_2 or O_3 have so far not predicted false positives of comparable strength to the modern Earth's photosynthetic biosphere. These mechanisms work predominantly for planets orbiting M dwarf stars, which are more amenable to transmission spectroscopy and which could also be observed using current and future ground-based telescopes with direct imaging and/or high-resolution spectroscopy capabilities (*e.g.,* Snellen *et al.,* 2013; Males *et al.,* 2014; Rodler and López-Morales, 2014; Quanz *et al.,* 2015; Crossfield, 2016; Lovis *et al.,* 2016). For the upcoming JWST mission, these false positives will either be too small to be detected with transmission spectroscopy, or telltale signs, such as abundant CO and CO_2, will likely be seen in the spectrum of the planet before the false-positive O_2 signal is detected (Schwieterman *et al.,* 2016a). The amount of atmospheric CH_4, or its absence, will also help identify these false positives (Domagal-Goldman *et al.,* 2014) but will likely be more challenging to detect or set limits on, especially in direct imaging.

Abiotic generation of strong O_3 may also occur for planets orbiting F dwarfs (Domagal-Goldman *et al.,* 2014). This may be of concern to direct imaging missions that observe in the UV only, but if visible measurements of O_3 and O_2 are also attempted, it may be possible to quantify the abiotically generated O_3 and discriminate it from the larger fraction expected from a productive photosynthetic biosphere.

Looking to the future, biosignature science must address two significant questions: ''How do we discover new potential biosignatures—especially those with higher probabilities of detection?'' and ''How do we increase our confidence in the interpretation of the more detectable candidates we do have?'' There are two main ways to address the first question, namely by looking for additional disequilibrium or other anomalous or unexpected planetary

processes (*e.g.,* Hitchcock and Lovelock, 1967; Krissansen-Totton *et al.,* 2016) or by systematically studying gases likely to be produced by life to understand their longevity in the planetary environment and whether or not they are likely to be detectable (*e.g.,* Segura *et al.,* 2003, 2005; Domagal-Goldman *et al.,* 2011; Grenfell *et al.,* 2012, 2014; Rugheimer *et al.,* 2013, 2015; Seager *et al.,* 2013a, 2013b). The first approach could be very powerful, as it will be largely independent of known metabolisms and will instead focus on identifying life as an anomalous planetary process. However, it has the disadvantage that the environment being studied would need to be observed and understood extremely well so that an anomalous process could be identified.

In the second approach, we must first choose a candidate biosignature gas to study, and there are several means to do this, including exploring Earth's current biosignatures. This initial approach has the advantages that we know these characteristics can be produced by life, that they are observed in the relevant environment, and that the survivability of the gas is already proven. The disadvantage is that these biosignatures are drawn from the environment of one planet and may not represent the diversity of biological processes and planetary environments on other worlds.

To expand the possible dominant metabolisms and habitable environments, while maintaining high levels of plausibility, we can also search the biological and geological records of the early Earth, which for this purpose serves as a suite of habitable, and yet alien, environments. Specifically, the early Earth provides geochemical evidence that different metabolisms originated, and were dominant, in different time periods and environments (*e.g.,* Stüeken *et al.,* 2015b), and we can work to understand their likely biosignatures from constraining the properties of these ancient environments (*e.g.,* Arney *et al.,* 2016) and understanding the organisms that remain today. The disadvantage again is that these biosignatures, although potentially more varied than those for modern Earth, are still ''Earth-centric.''

Another approach is to remain agnostic to biological source or planetary context and survey a very large array of chemically stable, relatively small molecules that are likely to be volatile in a planetary atmosphere (*e.g.,* Seager and Bains, 2015). The advantage of this approach is that it can initially be non-metabolism-specific and so may consider molecules that are not currently, or in the past, produced by life on Earth. The disadvantage is that the extremely large number of candidate gases produced by chemistry must still be winnowed down to the most likely to be produced by life, to survive in the environment, and to be observed. This selection process to choose the best candidates will still require the application of some level of Earth-centric knowledge. Understanding and identifying false positives for potential biosignature gases identified without biological or environmental context will also be extremely challenging.

Once a candidate gas is chosen as being likely to be produced by life using one of the above methods, it must then pass the gauntlets of survivability and detectability in the planetary environment. Future research in this area must be able to answer the following questions: Is the gas able to avoid the normal sinks in a planetary environment, including destruction by photochemistry, reaction with volcanic gases, reaction with the surface, or being dissolved into an ocean? Finally, and perhaps most importantly, is the candidate biosignature likely to modify the global environment of an extrasolar planet and so produce a sufficiently large signal to be detectable via transmission, secondary eclipse, phase curves, or direct imaging spectroscopy? Is it spectrally active in accessible wavelength regions, and is it clear of overlap with other common planetary species? An example of the power of this approach in generating a new biosignature was given by Domagal-Goldman *et al.* (2011), where a photochemical model was used to understand the buildup of gases in an anoxic, early-Earth-like atmosphere due to surface fluxes from a putative sulfur-dominated biosphere, irradiated by stars of different spectral type. The resulting biosignature was not, as expected, a biogenic sulfur gas such as dimethyl sulfide, but rather ethane, which was produced as a by-product of the photolytic destruction of the biogenic sulfur gases. Future work should use similar methods to explore the survivability and detectability of biosignature gases in a range of atmospheres and under different stellar illumination.

To answer the second significant question—on increasing our confidence in the interpretation of the biosignatures we do have—the depth to which the environmental context for O_2 has now been studied sets a new standard for the field of biosignatures that should also guide future work. While O_2 clearly has many advantages as a highly detectable biosignature, some may consider it no longer ''robust,'' because we now know of potential abiotic sources. However, the existence of abiotic sources is likely true, or should at least be assumed, for all proposed biosignatures, given the complexity and probable diversity of planetary environments. Understanding possible abiotic generation mechanisms puts us in a much stronger position when planning observations or interpreting exoplanet data. Following the example being developed for O_2, a thorough study of environmental lifetime, context, potential false positives, and the detectability of both biosignature and false-positive discriminators should be undertaken for all newly proposed biosignature candidates. These studies will enhance the robustness of proposed biosignatures and provide knowledge and observing strategies to increase confidence in biosignature detection.

For the specific example of biogenic O_2, it is now clear that the robustness of the detection will increase as potential false-positive mechanisms are ruled out by observations of other atmospheric gases or planetary environmental characteristics, and measurements of more of these can be obtained as the accessible wavelength range increases (Table 2). Discriminating the false positive due to water loss and the formation of massive O_2 atmospheres can be done with observations of O_4 absorption in the visible and NIR, requiring wavelength ranges from 0.4 to 1.0 μm for direct imaging and 0.6 to 1.3 μm for transmission. To search for the CH_4, CO, and CO_2, which will help discriminate several other possible abiotic mechanisms, observations out to 2.5 μm will be required, whereas observations out to 4.5 μm will be desirable to identify abiotic O_2 generated by water loss from a low inventory of noncondensable gases and to also pick up stronger CO_2 and CO bands to strengthen interpretation of some of the other false-positive mechanisms. If MIR observations are available, such as for ground-based direct imaging of M dwarf planets, then absorption from

Table 2. Spectral Features as a Function of Wavelength Range That Could Be Sought for Identification of an Oxygenic Photosynthetic Biosphere

Molecules/Feature	*0.2–1.8 μm*	*1.8–2.5 μm*	*2.5–5.0 μm*	*5.0–20 μm*	*Notes*
O_2	0.2, 0.69, 0.76, 1.27			—	Biosignature sought—also disequilibrium pair with CH_4, N_2O
O_3	0.2–0.3 (strong) 0.38–0.65			9.6	Biosignature sought
O_4 (O_2-O_2 CIA)[a]	0.45, 0.48, 0.53, 0.57, 0.63, 1.06, 1.27 (strong)			—	False-positive indicator—dense O_2 from ocean runaway. Schwieterman *et al.,* 2016a, 2016b
CH_4	0.79, 0.89, 1.0, 1.1, 1.4, 1.7	2.31 (strong)	3.3 (strong)	7.7	Biosignature sought—disequilibrium pair with O_2. Indicates presence of O_2 sink. Domagal-Goldman *et al.,* 2014
CO_2	1.05, 1.21, 1.6	2.01	4.2 (strong)	9.4, 10.4, 15	False positive indicator, esp. in combination with CO—ongoing CO_2 photolysis. Schwieterman *et al.,* 2016a; Wang *et al.,* 2016
CO	1.6	2.35			False-positive indicator, esp. in combination with CO_2—ongoing CO_2 photolysis. Schwieterman *et al.,* 2016a; Wang *et al.,* 2016
N_4 (N_2-N_2 CIA)[b]			4.1		False-positive discriminant—helps quantify noncondensable gas fraction, disequilibrium biosignature when paired with N_2/O_2. Schwieterman *et al.,* 2015a; Krissansen-Totton *et al.,* 2016
N_2O		2.11, 2.25	2.6, 2.67, 2.97, 3.6, 3.9, 4.3, 4.5	7.9, 17.0	Biosignature sought—disequilibrium pair with O_2
H_2	0.64–0.66, 0.8–0.85				Possible bulk atmospheric constituent
H_2O	0.65, 0.72, 0.82, 0.94, 1.12, 1.4	1.85, 2.5		6.3	Habitability indicator, false-positive discriminant—could show ocean loss or presence of catalyst for CO_2 recombination. Tian *et al.,* 2014; Gao *et al.,* 2015; Schwieterman *et al.,* 2016a,b
Ocean glint[c]	0.8–0.9 (optimal)				Habitability indicator, false-positive discriminant, disequilibrium biosignature when paired with O_2/N_2. Robinson *et al.,* 2010; Zugger *et al.,* 2011; Krissansen-Totton *et al.,* 2016
Vegetation red edge	0.6 (halophile)[d] 0.7 (photosynthesis—G dwarf)[e]				Biosignature sought. Kiang *et al.,* 2007b; Arnold, 2008; Schwieterman *et al.,* 2015a
Seasonal variability	CO_2 (1.6), CH_4 (1.1 and 1.4)			CO_2 (15)	Biosignature sought—seasonal variability in biomass building and metabolic output. Meadows, 2008

All values in the table are given in microns (μm).
[a]Hermans *et al.* (1999); Thalman and Volkamer (2013); Greenblatt *et al.* (1990); Maté *et al.* (1999).
[b]Lafferty *et al.* (1996).
[c]Robinson *et al.* (2010).
[d]Schwieterman *et al.* (2015a).
[e]Gates *et al.* (1965).
All other molecular band wavelengths in Table 2 derived from HITRAN; Rothman *et al.* (2013).

water vapor at 6.3 μm, CH_4 at 7.7 μm, O_3 at 9.6 μm, and CO_2 at 15 μm will also greatly help the interpretation of O_2 or O_3 as biosignatures (*e.g.,* Selsis *et al.,* 2002).

Finally, the studies to date have shown that potential false positives for life are inextricably tied to the planetary environment and will depend on planetary evolution and properties, the incoming stellar spectrum, and the planetary atmosphere's interaction with it. These studies have therefore also highlighted the importance of understanding the spectral characteristics of the host star and especially its UV spectrum and activity—work that needs to be done in the near-term before we lose UV-capable telescopes like the Hubble Space Telescope. Additional laboratory and field work to understand the origin and evolution of metabolisms on Earth, their output gases, and rates for key reactions that can serve as sources or sinks for abiotic oxygen, such as the rate of the aqueous recombination of CO and O in the oceans, is also needed to inform the search for life on exoplanets. To improve our understanding of potential sinks for abiotic O_2, we also need to better understand the photochemical cycles on Venus and incorporate catalytic reactions with chlorine into photochemical models of terrestrial exoplanets. Finally, to more accurately predict false-positive mechanisms and observable features for terrestrial exoplanets, our models of the interaction of the planetary atmosphere with stellar radiation will require improvements in gas molecular opacities, especially in the presence of other broadening gases, improved databases for collisionally induced absorption, and laboratory studies of haze and condensate formation and optical properties (*cf.* Fortney *et al.,* 2016).

6. Conclusions

Phototrophs have developed a metabolism that can capitalize on plentiful sunlight, abundant water, and the carbon dioxide in our atmosphere to dominate our planet's surface biosphere and significantly modify our planet's atmosphere. The atmospheric oxygen that photosynthesizers produce has many advantages as a biosignature for first-generation terrestrial planet characterization missions, including its relative abundance and uniform distribution throughout the atmospheric column. This allows O_2 to be visible in the presence of planetwide clouds and to be searched for in transmission observations that, due to refraction, may be limited to probing planetary stratospheres for signs of life. However, we now know that abundant oxygen or ozone in a planetary atmosphere could be produced by several abiotic mechanisms, including photolysis and atmospheric escape. These studies have advanced the field of biosignatures by identifying possible false positives and allowing us to explore how to avoid or identify an abiotic source of O_2—thereby increasing our confidence in biosignature detection. These mechanisms inform our choices of optimal targets and allow us to design better measurements to guard against false positives. In general, a better understanding of the environmental context of the detection is critical, including properties of the chemistry of the planet itself as well as the radiation from its host star.

Most of these mechanisms affect planets orbiting M dwarf stars and so will be relevant to missions such as JWST and to extremely large telescopes that will observe M dwarf exoplanets in transmission and direct imaging. Target selection of host stars more massive than 0.4 $M_\odot$ (M3V and earlier) and planets within the conservative habitable zone may help avoid planets with abundant abiotic O_2 due to water loss. Additionally, searching for the signs of strong O_4 or CO in the planetary spectrum, or the lack of H_2O or CH_4, could help discriminate between biological and abiotic sources of O_2 or O_3. Most abiotic mechanisms that produce O_2 or O_3 via photochemistry driven by the M dwarf host star spectrum are unlikely to produce signals strong enough to be readily detectable by first-generation exoplanet characterization missions either by transmission or direct imaging spectroscopy. For direct imaging observations, photochemical production of ozone for planets orbiting F dwarf stars, atmospheric loss near the inner edge of the habitable zone, or production of O_2 via photolysis in planetary atmospheres with low noncondensable gas fractions could produce the strongest false positives. In these cases, observations of O_3 and O_4 at visible wavelengths and quantification of O_4 or N_4 at NIR wavelengths could help rule out these scenarios.

In advance of telescopic observations, the future of biosignature research will focus on two key areas related to the identification of new biosignatures for study and research to enhance our confidence in biosignature interpretation through the vetting of these biosignatures for environmental lifetime, context, potential false positives, and detectability. Supporting laboratory and field work on biosignature gas sources and sinks, along with observations of the full spectrum of the host star, including the UV portion, will improve our ability to predict planetary photochemistry and discriminate between abiotic and biological sources for atmospheric gases. Near-term observations of "hot Earths," planets too close to their star to be habitable, may help illuminate terrestrial planet evolution and some of the proposed false-positive mechanisms. The recent detailed study of O_2 as a biosignature has shown us that to search for life on a distant world it is not enough to just detect O_2 or O_3 in the planetary atmosphere—other molecules, including O_4, CO, CO_2, CH_4, H_2O, and N_4 should also be sought, encouraging us to obtain the broadest wavelength range possible when characterizing potentially habitable extrasolar planets. Ultimately we have to not only observe gases in the spectrum of a distant planet but also recognize their significance and context in the planetary environment.

Acknowledgments

This work was performed as part of the NASA Astrobiology Institute's Virtual Planetary Laboratory research effort, supported by the National Aeronautics and Space Administration through the NASA Astrobiology Institute under solicitation NNH12ZDA002C and Cooperative Agreement number NNA13AA93A. I thank the entire VPL Team for their continued scientific input, support, creativity, hard work, and inspiration, without which this review would not have been possible. In particular I would like to thank Giada Arney, Roger Buick, David Crisp, Shawn Domagal-Goldman, Nancy Kiang, Andrew Lincowski, Rodrigo Luger, Niki Parenteau, Tyler Robinson, Eddie Schwieterman, and Kevin Zahnle for lending their considerable expertise through discussions and comments. I would also like to thank Ronald Hasler, Jacob Lustig-Yaeger, Eddie Schwieterman, Drake Deming, and Giada Arney for assistance in preparing the figures. Two referees provided thorough and

thoughtful comments that improved the quality of this manuscript, and I greatly appreciate their time and assistance.

Author Disclosure Statement

No competing financial interests exist.

References

Airapetian, V.S., Glocer, A., Gronoff, G., Hébrard, E., and Danchi, W. (2016) Prebiotic chemistry and atmospheric warming of early Earth by an active young Sun. *Nat Geosci* 9:452–455.

Albarède, F. (2009) Volatile accretion history of the terrestrial planets and dynamic implications. *Nature* 461:1227–1233.

Allen, D.A., Crisp, D., and Meadows, V.S. (1992) Variable oxygen airglow on Venus as a probe of atmospheric dynamics. *Nature* 359:516–519.

Anbar, A.D., Duan, Y., Lyons, T.W., Arnold, G.L., Kendall, B., Creaser, R.A., Kaufman, A.J., Gordon, G.W., Scott, C., Garvin, J., and Buick, R. (2007) A whiff of oxygen before the Great Oxidation Event? *Science* 317:1903–1906.

Anglada-Escudé, G., Amado, P.J., Barnes, J., Berdiñas, Z.M., Butler, R.P., Coleman, G.A., de la Cueva, I., Dreizler, S., Endl, M., Giesers, B. Jeffers, S.V., Jenkins, J.S., Jones, H.R., Kiraga, M., Kürster, M., López-González, M.J., Marvin, C.J., Morales., N., Morin, J., Nelson, R.P., Oritz, J.L., Ofir, A., Paardekooper, S.-J., Reiners, A., Rodríguez, E., Rodríguez-López, C., Sarmiento, L.F., Strachan, J.P., Tsapras, Y., Tuomi, M., and Zechmeister, M. (2016) A terrestrial planet candidate in a temperate orbit around Proxima Centauri. *Nature* 536:437–440.

Arney, G., Meadows, V., Crisp, D., Schmidt, S.J., Bailey, J., and Robinson, T. (2014) Spatially resolved measurements of H_2O, HCl, CO, OCS, SO_2, cloud opacity, and acid concentration in the Venus near-infrared spectral windows. *J Geophys Res: Planets* 119:1860–1891.

Arney, G., Domagal-Goldman, S.D., Meadows, V.S., Wolf, E.T., Schwieterman, E., Charnay, B., Claire, M., Hébrard, E., and Trainer, M.G., (2016) The pale orange dot: the spectrum and habitability of hazy Archean Earth. *Astrobiology* 16:873–899.

Arney, G.N., Meadows, V.S., Domagal-Goldman, S.D., Deming, D., Robinson, T.D., Tovar, G., Wolf, E.T., and Schwieterman, E. (2017) Pale orange dots: the impact of organic haze on the habitability and detectability of Earthlike exoplanets. *Astrophys J* 836, doi:10.3847/1538-4357/836/1/49.

Arnold L. (2008) Earthshine observation of vegetation and implication for life detection on other planets—a review of 2001–2006 works. *Space Sci Rev* 135:323–333.

Arnold, L., Gillet, S., Lardière O., Riaud, P., and Schneider, J. (2002) A test for the search for life on extrasolar planets: looking for the terrestrial vegetation signature in the Earthshine spectrum. *Astron Astrophys* 392:231–237.

Arnold, L., Ehrenreich, D., Vidal-Madjar, A., Dumusque, X., Nitschelm, C., Querel, R.R., Hedelt, P., Berthier, J., Lovis, C., Moutou, C., Ferlet, R., and Crooker, D. (2014) The Earth as an extrasolar transiting planet-II. HARPS and UVES detection of water vapour, biogenic O_2, and O_3. *Astron Astrophys* 564:A58.

Bacastow, R.B., Keeling, C.D., and Whorf, T.P. (1985) Seasonal amplitude increase in atmospheric CO_2 concentration at Mauna Loa, Hawaii, 1959–1982. *J Geophys Res* 90:10529–10540.

Baraffe, I., Chabrier, G., Allard, F., and Hauschildt, P.H. (1998) Evolutionary models for solar metallicity low-mass stars: mass-magnitude relationships and color-magnitude diagrams. *Astron Astrophys* 337:403–412.

Barnes, R., Meadows, V.S., and Evans, N. (2015) Comparative habitability of transiting exoplanets. *Astrophys J* 814, doi:10.1088/0004-637X/814/2/91.

Barnes, R., Deitrick, R., Luger, R., Driscoll, P.E., Quinn, T.R., Fleming, D.P., Guyer, B., McDonald, D.V., Meadows, V.S., Arney, G., Crisp, D., Domagal-Goldman, S.D., Lincowski, A., Lustig-Yaeger, J., and Schwieterman, E. (2016) The habitability of Proxima Centauri b I: evolutionary scenarios. arXiv:1608.06919

Bekker, A., Holland, H.D., Wang, P.-L., Rumble, D., Stein, H.J., Hannah, J.L., Coetzee, L.L., and Beukes, N.J. (2004) Dating the rise of atmospheric oxygen. *Nature* 427:117–120.

Berta-Thompson, Z.K., Irwin, J., Charbonneau, D., Newton, E.R., Dittmann, J.A., Astudillo-Defru, N., Bonfils, X., Gillon, M., Jehin, E., Stark, A.A., Stalder, B., Bouchy, F., Delfosse, X., Forveille, T., Lovis, C., Mayor, M., Neves, V., Pepe, F., Santos, N.C., Udry, S., and Wünsche, A. (2015) A rocky planet transiting a nearby low-mass star. *Nature* 527:204–207.

Bétrémieux, Y. and Kaltenegger, L. (2013) Transmission spectrum of Earth as a transiting exoplanet from the ultraviolet to the near-infrared. *Astrophys J* 772:L31.

Bétrémieux, Y. and Kaltenegger, L. (2014) Impact of atmospheric refraction: how deeply can we probe exo-Earth's atmospheres during primary eclipse observations? *Astrophys J* 791, doi:10.1088/0004-637X/791/1/7.

Beuzit, J.L., Feldt, M., Dohlen, K., Mouillet, D., Puget, P., Wildi, F., Abe, L., Antichi, J., Baruffolo, A., Baudoz, P., Boccaletti, A., Carbillet, M., Charton, J., Claudi, R., Downing, M., Fabron, C., Feautrier, P., Fedrigo, E., Fusco, T., Gach, J.-L., Gratton, R., Henning, T., Hubin, N., Joos, F., Kasper, M., Langlois, M., Lenzen, R., Moutou, C., Pavlov, A., Petit, C., Pragt, J., Rabou, P., Rigal, F., Roelfsema, R., Rousset, G., Saisse, M., Schmid, H.-M., Stadler, E., Thalmann, C., Turatto, M., Udry, U., Vakili, F., and Waters, R. (2008) SPHERE: a 'Planet Finder' instrument for the VLT. *Proc SPIE* 7014, doi:10.1117/12.790120.

Blamont, J. and Chassefière, E. (1993) First detection of ozone in the middle atmosphere of Mars from solar occultation measurements. *Icarus* 104:324–336.

Blankenship, R. (2010) Early evolution of photosynthesis. *Plant Physiol* 154:434–438.

Bolcar, M.R., Balasubramanian, K., Clampin, M., Crooke, J., Feinberg, L., Postman, M., Quijada, M., Rauscher, B., Redding, D., Rioux, N., Shaklan, S., Stahl, H.P., Stahle, C., and Thronson, H. (2015) Technology development for the advanced technology large aperture space telescope (ATLAST) as a candidate large UV-optical-infrared (LUVOIR) surveyor. *Proc SPIE* 9602, doi:10.1117/12.2188559.

Brandt, T.D. and Spiegel, D.S. (2014) Prospects for detecting oxygen, water, and chlorophyll on an exo-Earth. *Proc Natl Acad Sci USA* 111:13278–13283.

Brogi, M., De Kok, R.J., Albrecht, S., Snellen, I.A.G., Birkby, J.L., and Schwarz, H. (2016) Rotation and winds of exoplanet HD 189733 b measured with high-dispersion transmission spectroscopy. *Astrophys J* 817:106.

Buick, R. (2007) Did the Proterozoic 'Canfield Ocean' cause a laughing gas greenhouse? *Geobiology* 5:97–100.

Buick, R. (2008) When did oxygenic photosynthesis evolve? *Phil Trans R Soc Lond B: Biol Sci* 363:2731–2743.

Buick, R., Dunlop, J.S.R., and Groves, D.I. (1981) Stromatolite recognition in ancient rocks: an appraisal of irregularly laminated structures in an Early Archaean chert-barite unit from North Pole, Western Australia. *Alcheringa* 5:161–181.

Canfield, D.E. (2005) The early history of atmospheric oxygen: homage to Robert M. Garrels. *Annu Rev Earth Planet Sci* 33:1–36.

Cash, W. (2006) Detection of Earth-like planets around nearby stars using a petal-shaped occulter. *Nature* 442:51–53.

Catling, D. and Kasting, J.F. (2007) Planetary atmospheres and life. In *Planets and Life: The Emerging Science of Astrobiology,* edited by W.T. Sullivan and J.A. Baross, Cambridge University Press, Cambridge, UK, pp 91–116.

Catling, D.C., Zahnle, K.J., and McKay, C.P. (2001) Biogenic methane, hydrogen escape, and the irreversible oxidation of early Earth. *Science* 293:839–843.

Catling, D.C., Glein, C.R., Zahnle, K.J., and McKay, C.P. (2005) Why O_2 is required by complex life on habitable planets and the concept of planetary ''oxygenation time.'' *Astrobiology* 5:415–438.

Chapman, S. (1930) A theory of upper-atmosphere ozone. *Memoirs of the Royal Meteorological Society* 3:103–125.

Charnay, B., Meadows, V., Misra, A., Leconte, J., and Arney, G. (2015) 3D modeling of GJ1214b's atmosphere: formation of inhomogeneous high clouds and observational implications. *Astrophys J* 813:L1.

Chassefière, E. (1996a) Hydrodynamic escape of oxygen from primitive atmospheres: applications to the cases of Venus and Mars. *Icarus* 552:537–552.

Chassefière, E. (1996b) Hydrodynamic escape of hydrogen from a hot water-rich atmosphere: the case of Venus. *J Geophys Res* 101:26039–26056.

Connes, P., Noxon, J.F., Traub, W.A., and Carleton, N.P. (1979). O_2 $^1\Delta$ emission in the day and night airglow of Venus. *Astrophys J* 233:L29–L32.

Cottini, V., Ignatiev, N.I., Piccioni, G., Drossart, P., Grassi, D., and Markiewicz, W.J. (2012) Water vapor near the cloud tops of Venus from Venus Express/VIRTIS dayside data. *Icarus* 217:561–569.

Cowan, N.B., Abbot, D.S., and Voigt, A. (2012) A false positive for ocean glint on exoplanets: the latitude-albedo effect. *Astrophys J* 752:L3.

Cowan, N.B., Greene, T., Angerhausen, D., Batalha, N.E., Clampin, M., Colon, K., Crossfield, I.J.M., Fortney, J.J., Gaudi, B.S., Harrington, J., Iro, N., Lillie, C.F., Linsky, J.L., López-Morales, M., Mandel, A.M., and Stevenson, K.B., on behalf of Exo PAG SAG-10. (2015) Characterizing transiting planet atmospheres through 2025. *Publ Astron Soc Pac* 127, doi:10.1086/680855.

Crisp, D., Meadows, V.S., Bezard, B., Bergh, C., De Maillard, J.-P., and Mills, F.P. (1996) Ground-based near-infrared observations of the Venus nightside: 1.27 μm O_2 ($a^1\Delta_g$) airglow from the upper atmosphere. *J Geophys Res: Planets* 101:4577–4593.

Crossfield, I.J. (2016) Exoplanet atmospheres and giant ground-based telescopes. arXiv:1604.06458

Crowe, S.A., Døssing, L.N., Beukes, N.J., Bau, M., Kruger, S.J., Frei, R., and Canfield, D.E. (2013) Atmospheric oxygenation three billion years ago. *Nature* 501:535–538.

Czaja, A.D., Johnson, C.M., Roden, E.E., Beard, B.L., Voegelin, A.R., Nägler, T.F., Beukes, N.J., and Wille, M. (2012) Evidence for free oxygen in the Neoarchean ocean based on coupled iron–molybdenum isotope fractionation. *Geochim Cosmochim Acta* 86:118–137.

Dalcanton, J., Seager, S., Aigrain, S., Battel, S., Brandt, N., Conroy, C., Feinberg, L., Gezari, S., Guyon, O., Harris, W., and Hirata, C. (2015) From cosmic birth to living Earths: the future of UVOIR space astronomy. arXiv:1507.04779.

Dartnell, L. (2011) Biological constraints on habitability. *Astronomy & Geophysics* 52:25–28.

De Bergh, C., Bezard, B., Owen, T., Crisp, D., Maillard, J.P., and Lutz, B.L. (1991) Deuterium on Venus: observations from Earth. *Science* 251:547–549.

Deming, D. and Seager, S. (2009) Light and shadow from distant worlds. *Nature* 462:301–306.

Des Marais, D.J., Harwit, M.O., Jucks, K.W., Kasting, J.F., Lin, D.N., Lunine, J.I., Schneider, J., Seager, S., Traub, W.A., and Woolf, N.J. (2002) Remote sensing of planetary properties and biosignatures on extrasolar terrestrial planets. *Astrobiology* 2:153–181.

Domagal-Goldman, S.D. and Meadows, V.S. (2010) Abiotic buildup of ozone. In *Pathways Towards Habitable Planets,* edited by V. Coudé du Foresto, D.M. Gelino, and I. Ribas, Astronomical Society of the Pacific, San Francisco, p 152.

Domagal-Goldman, S.D., Meadows, V.S., Claire, M.W., and Kasting, J.F. (2011) Using biogenic sulfur gases as remotely detectable biosignatures on anoxic planets. *Astrobiology* 11: 419–441.

Domagal-Goldman, S.D., Segura, A., Claire, M.W., Robinson, T.D., and Meadows, V.S. (2014) Abiotic ozone and oxygen in atmospheres similar to prebiotic Earth. *Astrophys J* 792, doi:10.1088/0004-637X/792/2/90.

Driese, S.G., Jirsa, M.A., Ren, M., Brantley, S.L., Sheldon, N.D., Parker, D., and Schmitz, M. (2011) Neoarchean paleoweathering of tonalite and metabasalt: implications for reconstructions of 2.69 Ga early terrestrial ecosystems and paleoatmospheric chemistry. *Precambrian Res* 189:1–17.

Dutkiewicz, A., Volk, H., George, S.C., Ridley, J., and Buick, R. (2006) Biomarkers from Huronian oil-bearing fluid inclusions: an uncontaminated record of life before the Great Oxidation Event. *Geology* 34:437–440.

Etiope, G. and Sherwood Lollar, B. (2013) Abiotic methane on Earth. *Rev Geophys* 51:276–299.

Falkowski, P.G. and Godfrey, L.V. (2008) Electrons, life and the evolution of Earth's oxygen cycle. *Philos Trans R Soc Lond B Biol Sci* 363:2705–2716.

Farquhar, J., Bao, H., and Thiemens, M. (2000) Atmospheric influence of Earth's earliest sulfur cycle. *Science* 289:756–758.

Fast, K.E., Kostiuk, T., Lefèvre, F., Hewagama, T., Livengood, T.A., Delgado, J.D., Annen, J., and Sonnabend, G. (2009) Comparison of HIPWAC and Mars Express SPICAM observations of ozone on Mars 2006–2008 and variation from 1993 IRHS observations. *Icarus* 203:20–27.

Fortney, J.J., Robinson, T.D., Domagal-Goldman, S., Skålid Amundsen, D., Brogi, M., Claire, M., Crisp, D., Hebrard, E., Imanaka, H., de Kok, R., Marley, M.S., Teal, D., Barman, T., Bernath, P., Burrows, A., Charbonneau, D., Freedman, R.S., Gelino, D., Helling, C., Heng, K., Jensen, A.G., Kane, S., Kempton, E.M.-R., Kopparapu, R.K., Lewis, N.K., López-Morales, M., Lyons, J., Lyra, W., Meadows, V., Moses, J., Pierrehumbert, R., Venot, O., Wang, S.X., and Wright, J.T. (2016) The need for laboratory work to aid in the understanding of exoplanetary atmospheres. arXiv:1602.06305

France, K., Linsky, J.L., Tian, F., Froning, C.S., and Roberge, A. (2012) Time-resolved ultraviolet spectroscopy of the M dwarf GJ876 exoplanetary system. *Astrophys J* 750:L32.

France, K., Froning, C.S., Linsky, J.L., Roberge, A., Stocke, J.T., Tian, F., Bushinsky, R., Désert, J.-M., Mauas, P., Vieytes, M., and Walkowicz, L. (2013) The ultraviolet radiation environment around M dwarf exoplanet host stars. *Astrophys J* 763, doi:10.1088/0004-637X/763/2/149.

France, K., Parke Loyd, R.O., Youngblood, A., Brown, A., Schneider, P.C., Hawley, S.L., Froning, C.S., Linsky, J.L., Roberge, A., Buccino, A.P., Daveneport, J.R.A., Fontenla,

J.M., Kaltenegger, L., Kowalski, A.F., Mauas, P.J.D., Miguel, Y., Redfield, S., Rugheimer, S., Tian, F., Vieytes, M.C., Walkowicz, L.M., and Weisenburger, K.L. (2016) The MUSCLES treasury survey. I. Motivation and overview. *Astrophys J* 820, doi:10.3847/0004-637X/820/2/89.

Gao, P., Hu, R., Robinson, T.D., Li, C., and Yung, Y.L. (2015) Stabilization of CO_2 atmospheres on exoplanets around M dwarf stars. *Astrophys J* 806:249–261.

García Muñoz, A., Zapatero Osorio, M.R., Barrena, R., Montañés-Rodríguez, P., Martín, E.L., and Pallé, E. (2012) Glancing views of the Earth: from a lunar eclipse to an exoplanetary transit. *Astrophys J* 755, doi:10.1088/0004-637X/755/2/103.

Garvin, J., Buick, R., Anbar, A.D., Arnold, G.L., and Kaufman, A.J. (2009) Isotopic evidence for an aerobic nitrogen cycle in the latest Archean. *Science* 323:1045–1048.

Gates, D.M., Keegan, H.J., Schleter, J.C., and Weidner, V.R. (1965) Spectral properties of plants. *Appl Opt* 4:11–20.

George, S.C., Volk, H., Dutkiewicz, A., Ridley, J., and Buick, R. (2008) Preservation of hydrocarbons and biomarkers in oil trapped inside fluid inclusions for >2 billion years. *Geochim Cosmochim Acta* 72:844–870.

George, S.C., Dutkiewicz, A., Volk, H., Ridley, J., Mossman, D.J., and Buick, R. (2009) Oil-bearing fluid inclusions from the Palaeoproterozoic: a review of biogeochemical results from time-capsules >2.0 Ga old. *Science in China Series D: Earth Sciences* 52:1–11.

Gillon, M., Jehin, E., Lederer, S.M., Delrez, L., de Wit, J., Burdanov, A., Van Grootel, V., Burgasser, A.J., Triaud, A.H., Opitom, C., and Demory, B.O. (2016) Temperate Earth-sized planets transiting a nearby ultracool dwarf star. *Nature* 533: 221–224.

Gillon, M., Triaud, A.H., Demory, B.O., Jehin, E., Agol, E., Deck, K.M., Lederer, S.M., de Wit, J., Burdanov, A., Ingalis, J.G., Bolmont, E., Leconte, J., Raymond, S.N., Selsis, F., Turbet, M., Barkaoui, K., Burgasser, A., Burleigh, M.R., Carey, S.J., Chaushev, A., Copperwheat, C.M., Delrez, L., Fernandes, C.S., Holdsworth, D.L., Kotze, E.J., *et al.* (2017) Seven temperate terrestrial planets around the nearby ultracool dwarf star TRAPPIST-1. *Nature* 542:456–460.

Greenblatt, G.D., Orlando, J.J., Burkholder, J.B., and Ravishankara, A.R. (1990) Absorption measurements of oxygen between 330 and 1140 nm. *J Geophys Res: Atmospheres* 95:18577–18582.

Greene, T.P., Line, M.R., Montero, C., Fortney, J.J., Lustig-Yaeger, J., and Luther, K. (2016) Characterizing transiting exoplanet atmospheres with JWST. *Astrophys J* 817, doi:10.3847/0004-637X/817/1/17.

Grenfell, J.L., Stracke, B., von Paris, P., Patzer, B., Titz, R., Segura, A., and Rauer, H. (2007) The response of atmospheric chemistry on earthlike planets around F, G and K Stars to small variations in orbital distance. *Planet Space Sci* 55:661–671.

Grenfell, J.L., Grießmeier, J.M., von Paris, P., Patzer, A.B.C., Lammer, H., Stracke, B., Gebauer, S., Schreier, F., and Rauer, H. (2012) Response of atmospheric biomarkers to NOx-induced photochemistry generated by stellar cosmic rays for Earth-like planets in the habitable zone of M dwarf stars. *Astrobiology* 12:1109–1122.

Grenfell, J.L., Gebauer, S., Paris, P.V., Godolt, M., and Rauer, H. (2014) Sensitivity of biosignatures on Earth-like planets orbiting in the habitable zone of cool M-dwarf stars to varying stellar UV radiation and surface biomass emissions. *Planet Space Sci* 98:66–76.

Grinspoon, D.H. (1993) Implications of the high D/H ratio for the sources of water in Venus' atmosphere. *Nature* 363:428–431.

Guzmán-Marmolejo, A., Segura, A., and Escobar-Briones, E. (2013) Abiotic production of methane in terrestrial planets. *Astrobiology* 13:550–559.

Hamano, K., Abe, Y., and Genda, H. (2013) Emergence of two types of terrestrial planet on solidification of magma ocean. *Nature* 497:607–610.

Harman, C.E., Schwieterman, E.W., Schottelkotte, J.C., and Kasting, J.F. (2015) Abiotic O_2 levels on planets around F, G, K, and M stars: possible false positives for life? *Astrophys J* 812, doi:10.1088/0004-637X/812/2/137.

Hawley, S.L., Allred, J.C., Johns-Krull, C.M., Fisher, G.H., Abbett, W.P., Alexseev, I., Avgoloupis, S.I., Deustua, S.E., Gunn, A., Seiradakis, J.H., Sirk, M.M, and Valenti, J.A. (2003) Multiwavelength observations of flares on AD Leonis. *Astrophys J* 597:535–554.

Hedelt, P., von Paris, P., Godolt, M., Gebauer, S., Grenfell, J.L., Rauer, H., Shreier, F., Selsis, F., and Trautmann, T. (2013) Spectral features of Earth-like planets and their detectability at different orbital distances around F, G, and K-type stars. *Astron Astrophys* 553:A9.

Hedges, S.B., Blair, J.E., Venturi, M.L., and Shoe, J.L. (2004) A molecular timescale of eukaryote evolution and the rise of complex multicellular life. *BMC Evol Biol* 4, doi:10.1186/1471-2148-4-2.

Hegde, S., Paulino-Lima, I.G., Kent, R., Kaltenegger, L., and Rothschild, L. (2015) Surface biosignatures of exo-Earths: remote detection of extraterrestrial life. *Proc Natl Acad Sci USA* 112:3886–3891.

Hennessy, J., Balasubramanian, K., Moore, C.S., Jewell, A.D., Nikzad, S., France, K., and Quijada, M. (2016) Performance and prospects of far ultraviolet aluminum mirrors protected by atomic layer deposition. *J Astron Telesc Instrum Syst* 2, doi:10.1117/1.JATIS.2.4.041206.

Henry, T.J., Jao, W.-C., Winters, J.G., Dieterich, S., Finch, C.T., Hambly, N.C., Ianna, P.A., McCarthy, D.W., Riedel, A.R., Subasavage, J.P., and the RECONS Team. (2016) The census of objects within 10 parsecs [id. 142.01]. In *AAS Meeting Abstracts*, #227, American Astronomical Society, Washington, DC.

Hermans, C., Vandaele, A.C., Carleer, M., Fally, S., Colin, R., Jenouvrier, A., Coquart, B., and Mérienne, M.F. (1999) Absorption cross-sections of atmospheric constituents: NO_2, O_2, and H_2O. *Environmental Science and Pollution Research* 6: 151–158.

Hitchcock, D.R. and Lovelock, J.E. (1967) Life detection by atmospheric analysis. *Icarus* 7:149–159.

Hohmann-Marriott, M.F. and Blankenship, R.E. (2012) The photosynthetic world. In *Photosynthesis: Plastid Biology, Energy Conversion and Carbon Assimilation,* edited by J.J. Eaton-Rye, B.C. Tripathy, and T.D. Sharkey, Springer, Dordrecht, the Netherlands, pp 3–32.

Hu, R. and Seager, S. (2014) Photochemistry in terrestrial exoplanet atmospheres. III. Photochemistry and thermochemistry in thick atmospheres on super Earths and mini Neptunes. *Astrophys J* 784, doi:10.1088/0004-637X/784/1/63.

Hu, R., Seager, S., and Bains, W. (2012) Photochemistry in terrestrial exoplanet atmospheres. I. Photochemistry model and benchmark cases. *Astrophys J* 761, doi:10.1088/0004-637X/761/2/166.

Hunten, D.M. (1993) Atmospheric evolution of the terrestrial planets. *Science* 259:915.

Ingersoll, A.P. (1969) The runaway greenhouse: a history of water on Venus. *Journal of the Atmospheric Sciences* 26: 1191–1198.

Johnson, B. and Goldblatt, C. (2015) The nitrogen budget of Earth. *Earth-Science Reviews* 148:150–173.

Johnston, H.S. (1975) Global ozone balance in the natural stratosphere. *Rev Geophys* 13:637–649.

Kaltenegger, L., Traub, W.A., and Jucks, K.W. (2007) Spectral evolution of an Earth-like planet. *Astrophys J* 658:598.

Kane, S.R., Kopparapu, R.K., and Domagal-Goldman, S.D. (2014) On the frequency of potential Venus analogs from Kepler data. *Astrophys J* 794:L5.

Kasting, J.F. (1988) Runaway and moist greenhouse atmospheres and the evolution of Earth and Venus. *Icarus* 74:472–494.

Kasting, J.F. (1993) Earth's early atmosphere. *Science* 259: 920–926.

Kasting, J.F. (1997) Habitable zones around low mass stars and the search for extraterrestrial life. In *Planetary and Interstellar Processes Relevant to the Origins of Life,* edited by D.C.B. Whittet, Springer, Dordrecht, the Netherlands, pp 291–307.

Kasting, J.F. (2001) The rise of atmospheric oxygen. *Science* 293:819–820.

Kasting, J.F. and Catling, D. (2003) Evolution of a habitable planet. *Annu Rev Astron Astrophys* 41:429–463.

Kasting, J.F. and Donahue, T.M. (1980) The evolution of the atmospheric ozone. *J Geophys Res* 85:3255–3263.

Kasting, J.F., Whitmire, D.P., and Reynolds, R.T. (1993) Habitable zones around main sequence stars. *Icarus* 101:108–128.

Kasting, J.F., Kopparapu, R., Ramirez, R.M., and Harman, C.E. (2014) Remote life-detection criteria, habitable zone boundaries, and the frequency of Earth-like planets around M and late K stars. *Proc Natl Acad Sci USA* 111:12641–12646.

Kaufman, A.J., Johnston, D.T., Farquhar, J., Masterson, A.L., Lyons, T.W., Bates, S., Anbar, A.D., Arnold, G.L., Garvin, J., and Buick, R. (2007) Late Archean biospheric oxygenation and atmospheric evolution. *Science* 317:1900–1903.

Kawahara, H., Matsuo, T., Takami, M., Fujii, Y., Kotani, T., Murakami, N., Tamura, M., and Guyon, O. (2012) Can ground-based telescopes detect the oxygen 1.27 μm absorption feature as a biomarker in exoplanets? *Astrophys J* 758, doi:10.1088/0004-637X/758/1/13.

Keeling, C.D., Bacastow, R.B., Bain Bridge, A.E., Ekdahl, C.A., Jr., Guenther, P.R., Waterman, L.S., and Chin, J.F.S. (1976) Atmospheric carbon dioxide variations at Mauna Loa Observatory, Hawaii. *Tellus* 28:538–551.

Keeling, C.D., Chin, J.F.S., and Whorf, T.P. (1996) Increased activity of northern vegetation inferred from atmospheric CO_2 measurements. *Nature* 382:146–149.

Kelley, D.S., Karson, J.A., Früh-Green, G.L., Yoerger, D.R., Shank, T.M., Butterfield, D.A., Hayes, J.M., Schrenk, M.O., Olson, E.J., Proskurowski, G., and Jakuba, M. (2005) A serpentinite-hosted ecosystem: the Lost City hydrothermal field. *Science* 307:1428–1434.

Kharecha, P., Kasting, J., and Siefert, J. (2005) A coupled atmosphere-ecosystem model of the early Archean Earth. *Geobiology* 3:53–76.

Kiang, N.Y. (2014) Looking for life elsewhere: photosynthesis and astrobiology. *Biochemist* 36:24–30.

Kiang, N.Y., Siefert, J., Govindjee, and Blankenship, R.E. (2007a) Spectral signatures of photosynthesis. I. Review of Earth organisms. *Astrobiology* 7:222–251.

Kiang, N.Y., Segura, A., Tinetti, G., Govindjee, Blankenship, R.E., Cohen, M., Siefert, J., Crisp, D., and Meadows, V.S. (2007b) Spectral signatures of photosynthesis. II. Coevolution with other stars and the atmosphere on extrasolar worlds. *Astrobiology* 7:252–274.

Kopparapu, R.K., Ramirez, R., Kasting, J.F., Eymet, V., Robinson, T.D., Mahadevan, S., Terrien, R.C., Domagal-Goldman, S., Meadows, V., and Deshpande, R. (2013) Habitable zones around main-sequence stars: new estimates. *Astrophys J* 765, doi:10.1088/0004-637X/765/2/131.

Kopparapu, R.K., Ramirez, R.M., SchottelKotte, J., Kasting, J.F., Domagal-Goldman, S., and Eymet, V. (2014) Habitable zones around main-sequence stars: dependence on planetary mass. *Astrophys J* 787:L29.

Krasnopolsky, V.A. (2010) Spatially resolved high-resolution spectroscopy of Venus 1. Variations of CO_2, CO, HF, and HCl at the cloud tops. *Icarus* 208:539–547.

Kreidberg, L., Bean, J.L., Désert, J.-M., Benneke, B., Deming, D., Stevenson, K.B., Seager, S., Berta-Thompson, Z., Seifahrt, A., and Homeier, D. (2014) Clouds in the atmosphere of the super-Earth exoplanet GJ 1214b. *Nature* 505:69–72.

Krissansen-Totton, J., Bergsman, D., and Catling, D.C. (2016) On detecting biospheres from chemical thermodynamic disequilibrium in planetary atmospheres. *Astrobiology* 16:39–67.

Kump, L.R. (2008) The rise of atmospheric oxygen. *Nature* 451: 277–278.

Lafferty, W.J., Solodov, A.M., Weber, A., Olson, W.B., and Hartmann, J.M. (1996) Infrared collision-induced absorption by N_2 near 4.3 μm for atmospheric applications: measurements and empirical modeling. *Appl Opt* 35:5911–5917.

Leconte, J., Forget, F., Charnay, B., Wordsworth, R., and Pottier, A. (2013) Increased insolation threshold for runaway greenhouse processes on Earth-like planets. *Nature* 504:268–271.

Lederberg, J. (1965) Signs of life. *Nature* 207:9–13.

Léger, A., Fontecave, M., Labeyrie, A., Samuel, B., Demangeon, O., and Valencia, D. (2011) Is the presence of oxygen on an exoplanet a reliable biosignature? *Astrobiology* 11:335–341.

Liang, M.-C., Hartman, H., Kopp, R.E., Kirschvink, J.L., and Yung, Y.L. (2006) Production of hydrogen peroxide in the atmosphere of a snowball Earth and the origin of oxygenic photosynthesis. *Proc Natl Acad Sci USA* 103:18896–18899.

Linsky, J.L., France, K., and Ayres, T. (2013) Computing intrinsic Lyα fluxes of F5 V to M5 V stars. *Astrophys J* 766, doi:10.1088/0004-637X/766/2/69.

Lissauer, J.J. (2007) Planets formed in habitable zones of M dwarf stars probably are deficient in volatiles. *Astrophys J* 660:L149–L152.

Lovelock, J.E. (1965) A physical basis for life detection experiments. *Nature* 207:568–570.

Lovelock, J.E. (1975) Thermodynamics and the recognition of alien biospheres. *Proc R Soc Lond B Biol Sci* 189:167–181.

Lovis, C., Snellen, I., Mouillet, D., Pepe, F., Wildi, F., Astudillo-Defru, N., Beuzit, J.-L., Bonfils, X., Cheetham, A., Conod, U., Delfosse, X., Ehrenreich, D., Figueira, P., Forveille, T., Martins, J.H.C., Quanz, S., Santos, N.C., Schmid, H.-M., Ségransan, D., and Udry, S. (2016) Atmospheric characterization of Proxima b by coupling the SPHERE high-contrast imager to the ESPRESSO spectrograph. arXiv:1609.03082

Loyd, R.O.P., France, K., Youngblood, A., Schneider, P.C., Brown, A., Hu, R., Linsky, J.L., Froning, C.S., Redfield, S., Rugheimer, S., and Tian, F. (2016) The MUSCLES Treasury Survey. III. X-ray to infrared spectra of 11 M and K stars hosting planets. *Astrophys J* 824, doi:10.3847/0004-637X/824/2/102.

Luger, R. and Barnes, R. (2015) Extreme water loss and abiotic O_2 buildup on planets throughout the habitable zones of M dwarfs. *Astrobiology* 15:119–143.

Luo, G., Ono, S., Beukes, N.J., Wang, D.T., Xie, S., and Summons, R.E. (2016) Rapid oxygenation of Earth's atmosphere 2.33 billion years ago. *Sci Adv* 2, doi:10.1126/sciadv.1600134.

Lyons, T.W., Reinhard, C.T., and Planavsky, N.J. (2014) The rise of oxygen in Earth's early ocean and atmosphere. *Nature* 506:307–315.

Males, J.R., Close, L.M., Guyon, O., Morzinski, K., Puglisi, A., Hinz, P., Follette, K.B., Monnier, J.D., Tolls, V., Rodigas, T.J., Weinberger, A., Boss, A., Kopon, D., Wu, Y.-L., Esposito, S., Riccardi, A., Xompero, M., Briguglio, R., and Pinna, E. (2014) Direct imaging of exoplanets in the habitable zone with adaptive optics. *Proc SPIE* 9148, doi:10.1117/12.2057135.

Mancinelli, R.L. and Banin, A. (2003) Where is the nitrogen on Mars? *International Journal of Astrobiology* 2:217–225.

Marty, B., Zimmermann, L., Pujol, M., Burgess, R., and Philippot, P. (2013) Nitrogen isotopic composition and density of the Archean atmosphere. *Science* 342:101–104.

Maté, B., Lugez, C., Fraser, G.T., and Lafferty, W.J. (1999) Absolute intensities for the O_2 1.27 μm continuum absorption. *J Geophys Res: Atmospheres* 104:30585–30590.

McElroy, M.B. (1972) Mars: an evolving atmosphere. *Science* 175:443–445.

McElroy, M.B., Sze, N.D., and Yung, Y.L. (1973) Photochemistry of the Venus atmosphere. *Journal of the Atmospheric Sciences* 30:1437–1447.

Meadows, V. and Crisp, D. (1996) Ground-based near-infrared observations of the Venus nightside: the thermal structure and water abundance near the surface. *J Geophys Res: Planets* 101:4595–4622.

Meadows, V. and Seager, S. (2010) Terrestrial planet atmospheres and biosignatures. In *Exoplanets*, edited by S. Seager, University of Arizona Press, Tucson, pp 441–470.

Meadows, V.S. (2005) Modelling the diversity of extrasolar terrestrial planets. *Proceedings of the International Astronomical Union* 1:25–34.

Meadows, V.S. (2008) Planetary environmental signatures of habitability and life. In: *Exoplanets: detection, formation, properties, habitability*, Mason, J. (Ed.), Springer Science & Business Media.

Meadows, V.S., Arney, G.N., Schwieterman, E.W., Lustig-Yaeger, J., Lincowski, A.P., Robinson, T., Domagal-Goldman, S.D., Barnes, R.K., Fleming, D.P., Deitrick, R., and Luger, R. (2016) The habitability of Proxima Centauri b: II: Environmental states and observational discriminants. arXiv:1608.08620

Mennesson, B., Gaudi, S., Seager, S., Cahoy, K., Domagal-Goldman, S., Feinberg, L., Guyon, O., Kasdin, J., Marois, C., Mawet, D., Tamura, M., Mouillet, D., Prusti, T., Quirrenbach, A., Robinson, T., Rogers, L., Scowen, P., Somerville, R., Stapelfeldt, K., Stern, D., Still, M., Turnbull, M., Booth, J., Kiessling, A., Kuan, G., and Warfield, K. (2016) The Habitable Exoplanet (HabEx) Imaging Mission: preliminary science drivers and technical requirements. *Proc SPIE* 9904, doi:10.1117/12.2240457.

Mills, F.P. (1999) A spectroscopic search for molecular oxygen in the Venus middle atmosphere. *J Geophys Res: Planets* 104:30757–30763.

Mills, F.P. and Allen, M. (2007) A review of selected issues concerning the chemistry in Venus' middle atmosphere. *Planet Space Sci* 55:1729–1740.

Misra, A., Meadows, V., Claire, M., and Crisp, D. (2014a) Using dimers to measure biosignatures and atmospheric pressure for terrestrial exoplanets. *Astrobiology* 14:67–86.

Misra, A., Meadows, V., and Crisp, D. (2014b) The effects of refraction on transit transmission spectroscopy: application to Earth-like exoplanets. *Astrophys J* 792, doi:10.1088/0004-637X/792/1/61.

Montañés-Rodríguez, P., Pallé, E., Goode, P.R., and Martín-Torres, F.J. (2006) Vegetation signature in the observed globally integrated spectrum of Earth considering simultaneous cloud data: applications for extrasolar planets. *Astrophys J* 651, doi:10.1086/507694.

Montmessin, F., Bertaux, J.L., Lefèvre, F., Marcq, E., Belyaev, D., Gérard, J.C., Korablev, O., Fedorova, A., Sarago, V., and Vandaele, A.C. (2011) A layer of ozone detected in the nightside upper atmosphere of Venus. *Icarus* 216:82–85.

Narita, N., Enomoto, T., Masaoka, S., and Kusakabe, N. (2015) Titania may produce abiotic oxygen atmospheres on habitable exoplanets. *Sci Rep* 5, doi:10.1038/srep13977.

Nutman, A.P., Bennett, V.C., Friend, C.R., Van Kranendonk, M.J., and Chivas, A.R. (2016) Rapid emergence of life shown by discovery of 3,700-million-year-old microbial structures. *Nature* 537:535–538.

Olson, J.M. and Pierson, B.K. (1986) Photosynthesis 3.5 thousand million years ago. *Photosynth Res* 9:251–259.

Oren, A. (2015) Cyanobacteria in hypersaline environments: biodiversity and physiological properties. *Biodivers Conserv* 24:781–798.

Pace, G. and Pasquini, L. (2004) The age-activity-rotation relationship in solar-type stars. *Astron Astrophys* 426:1021–1034.

Painter, T.H., Duval, B., Thomas, W.H., Mendez, M., Heintzelman, S., and Dozier, J. (2001) Detection and quantification of snow algae with an airborne imaging spectrometer. *Appl Environ Microbiol* 67:5267–5272.

Pallé, E., Osorio, M.R.Z., Barrena, R., Montañés-Rodríguez, P., and Martín, E.L. (2009) Earth's transmission spectrum from lunar eclipse observations. *Nature* 459:814–816.

Pavlov, A., Brown, L., and Kasting, J. (2001) UV shielding of NH_3 and O_2 by organic hazes in the Archean atmosphere. *J Geophys Res: Planets* 106:23267–23287.

Pernice, H., Garcia, P., Willner, H., Francisco, J.S., Mills, F.P., Allen, M., and Yung, Y.L. (2004) Laboratory evidence for a key intermediate in the Venus atmosphere: peroxychloroformyl radical. *Proc Natl Acad Sci USA* 101:14007–14010.

Peters, B., Casciotti, K.L., Samarkin, V.A., Madigan, M.T., Schutte, C.A., and Joye, S.B. (2014) Stable isotope analyses of NO^{2-}, NO^{3-}, and N_2O in the hypersaline ponds and soils of the McMurdo Dry Valleys, Antarctica. *Geochim Cosmochim Acta* 135:87–101.

Pierrehumbert, R. and Gaidos, E. (2011) Hydrogen greenhouse planets beyond the habitable zone. *Astrophys J Lett* 734:L13.

Pilcher, C.B. (2003) Biosignatures of early Earth. *Astrobiology* 3:471–486.

Planavsky, N.J., Asael, D., Hofman, A., Reinhard, C.T., Lalonde, S.V., Knudsen, A., Wang, X., Ossa, F.O., Pecoits, E., Smith, A.J., and Beukes, N.J. (2014a) Evidence for oxygenic photosynthesis half a billion years before the Great Oxidation Event. *Nat Geosci* 7:283–286.

Planavsky, N.J., Reinhard, C.T., Wang, X., Thomson, D., McGoldrick, P., Rainbird, R.H., Johnson, T., Fischer, W.W., and Lyons, T.W. (2014b) Low Mid-Proterozoic atmospheric oxygen levels and the delayed rise of animals. *Science* 346: 635–638.

Quanz, S.P., Crossfield, I., Meyer, M.R., Schmalzl, E., and Held, J. (2015) Direct detection of exoplanets in the 3–10 μm range with E-ELT/METIS. *International Journal of Astrobiology* 14:279–289.

Ratner, M.I. and Walker, J.C. (1972) Atmospheric ozone and the history of life. *Journal of the Atmospheric Sciences* 29: 803–808.

Rauer, H., Gebauer, S., von Paris, P., Cabrera, J., Godolt, M., Grenfell, J.L., Belu, A., Selsis, F., Hedelt, P., and Schreier, F. (2011) Potential biosignatures in super-Earth atmospheres. I. Spectral appearance of super-Earths around M dwarfs. *Astron Astrophys* 529:A8.

Raymond, S.N., Scalo, J., and Meadows, V.S. (2007) A decreased probability of habitable planet formation around low-mass stars. *Astrophys J* 669:606–614.

Raymond, S.N., Barnes, R., and Mandell, A.M. (2008) Observable consequences of planet formation models in systems with close-in terrestrial planets. *Mon Not R Astron Soc* 384:663–674.

Reinhard, C.T., Planavsky, N.J., Olson, S.L., Lyons, T.W., and Erwin, D.H. (2016) Earth's oxygen cycle and the evolution of animal life. *Proc Natl Acad Sci USA* 113:8933–8938.

Riaud, P. and Schneider, J. (2007) Improving Earth-like planets' detection with an ELT: the differential radial velocity experiment. *Astron Astrophys* 469:355–361.

Ribas, I., Bolmont, E., Selsis, F., Reiners, A., Leconte, J., Raymond, S.N., Engle, S.G., Guinan, E.F., Morin, J., Turbet, M., Forget, F., and Anglada-Escudé, G. (2016) The habitability of Proxima Centauri b—I. Irradiation, rotation and volatile inventory from formation to the present. *Astron Astrophys* 596:A111.

Richard, C., Gordon, I.E., Rothman, L.S., Abel, M., Frommhold, L., Gustafsson, M., Hartmann, J.M., Hermans, C., Lafferty, W.J., Orton, G.S., Smith, K.M., and Tran, H. (2012) New section of the HITRAN database: collision-induced absorption (CIA). *J Quant Spectrosc Radiat Transf* 113:1276–1285.

Riding, R., Fralick, P., and Liang, L. (2014) Identification of an Archean marine oxygen oasis. *Precambrian Res* 251:232–237.

Rioux, N., Thronson, H., Feinberg, L., Stahl, H.P., Redding, D., Jones, A., Sturm, J., Collins, C. and Liu, A. (2015) A future large-aperture UVOIR space observatory: reference designs. *Proc SPIE* 9602, doi:10.1117/12.2187758.

Robinson, T.D., Meadows, V.S., and Crisp, D. (2010) Detecting oceans on extrasolar planets using the glint effect. *Astrophys J* 721:L67–L71.

Robinson, T.D., Ennico, K., Meadows, V.S., Sparks, W., Bussey, D.B.J., Schwieterman, E.W., and Breiner, J. (2014) Detection of ocean glint and ozone absorption using LCROSS Earth observations. *Astrophys J* 787, doi:10.1088/0004-637X/787/2/171.

Robinson, T.D., Stapelfeldt, K.R., and Marley, M.S. (2016) Characterizing rocky and gaseous exoplanets with 2 m class space-based coronagraphs. *Publ Astron Soc Pac* 128, doi:10.1088/1538-3873/128/960/025003.

Rodler, F. and López-Morales, M. (2014) Feasibility studies for the detection of O_2 in an Earth-like exoplanet. *Astrophys J* 781, doi:10.1088/0004-637X/781/1/54.

Rosenqvist, J. and Chassefiére, E. (1995) Inorganic chemistry of O_2 in dense planetary atmospheres. *Planet Space Sci* 43:3–10.

Rothman, L.S., Gordon, I.E., Babikov, Y., Barbe, A., Chris Benner, D., Bernath, P.F., Birk, M., Bizzocchi, L., Boudon, V., Brown, L.R., Campargue, A., Chance, K., Cohen, E.A., Coudert, L.H., Devi, V.M., Drouin, B.J., Fayt, A., Flaud, J.-M., Gamache, R.R., Harrison, J.J., Hartmann, J.-M., Hill, C., Hodges, J.T., Jacquemart, D., Jolly, A., Lamouroux, J., LeRoy, R.J., Li, G., Long, D.A., Lyulin, O.M., Mackie, C.J., Massie, S.T., Mikhailenko, S., Müller, H.S.P., Naumenko, O.V., Nikitin, A.V., Orphal, J., Perevalov, V., Perrin, A., Polovtseva, E.R., Richard, C., Smith, M.A.H., Starikova, E., Sung, K., Tashkun, S., Tennyson, J., Toon, G.C., Tyuterev, Vl.G., and Wagner, G. (2013) The HITRAN2012 molecular spectroscopic database. *J Quant Spectrosc Radiat Transf* 130:4–50.

Rubasinghege, G., Spak, S.N., Stanier, C.O., Carmichael, G.R., and Grassian, V.H. (2011) Abiotic mechanism for the formation of atmospheric nitrous oxide from ammonium nitrate. *Environ Sci Technol* 45:2691–2697.

Rugheimer, S., Kaltenegger, L., Zsom, A., Segura, A., and Sasselov, D. (2013) Spectral fingerprints of Earth-like planets around FGK stars. *Astrobiology* 13:251–269.

Rugheimer, S., Kaltenegger, L., Segura, A., Linsky, J., and Mohanty, S. (2015) Effect of UV radiation on the spectral fingerprints of Earth-like planets orbiting M stars. *Astrophys J* 809, doi:10.1088/0004-637X/809/1/57.

Sagan, C., Thompson, W.R., Carlson, R., Gurnett, D., and Hord, C. (1993) A search for life on Earth from the Galileo spacecraft. *Nature* 365:715–721.

Samarkin, V.A., Madigan, M.T., Bowles, M.W., Casciotti, K.L., Priscu, J.C., McKay, C.P., and Joye, S.B. (2010) Abiotic nitrous oxide emission from the hypersaline Don Juan Pond in Antarctica. *Nat Geosci* 3:341–344.

Sander, S.P., Friedl, R.R., Golden, D.M., Kurylo, M.J., Moortgat, G.K., Wine, P.H., Ravishankara, A.R., Kolb, C.E., Molina, M.J., Finlayson-Pitts, B.J., and Huie, R.E. (2006) *Chemical Kinetics and Photochemical Data for Use in Atmospheric Studies Evaluation Number 15,* JPL Publication 06-2, Jet Propulsion Laboratory, California Institute of Technology, Pasadena, CA. Available online at http://ntrs.nasa.gov/search.jsp?R=20090033862

Sanromá, E., Pallé, E., and García Muñoz, A. (2013) On the effects of the evolution of microbial mats and land plants on the Earth as a planet. Photometric and spectroscopic light curves of paleo-Earths. *Astrophys J* 766, doi:10.1088/0004-637X/766/2/133.

Sanromá, E., Pallé, E., Parenteau, M.N., Kiang, N.Y., Gutiérrez-Navarro, A.M., López, R., and Montañes-Rodríguez, P. (2014) Characterizing the purple Earth: modeling the globally integrated spectral variability of the Archean Earth. *Astrophys J* 780, doi:10.1088/0004-637X/780/1/52.

Schaefer, L., Wordsworth, R.D., Berta-Thompson, Z., and Sasselov, D. (2016) Predictions of the atmospheric composition of GJ 1132b. *Astrophys J* 829, doi:10.3847/0004-637X/829/2/63.

Schindler, T.L. and Kasting, J.F. (2000) Synthetic spectra of simulated terrestrial atmospheres containing possible biomarker gases. *Icarus* 145:262–271.

Schulze-Makuch, D., Méndez, A., Fairén, A.G., von Paris, P., Turse, C., Boyer, G., Davila, A.F., António, M.R.D.S., Catling, D., and Irwin, L.N. (2011) A two-tiered approach to assessing the habitability of exoplanets. *Astrobiology* 11:1041–1052.

Schwieterman, E.W., Cockell, C.S., and Meadows, V.S. (2015a) Nonphotosynthetic pigments as potential biosignatures. *Astrobiology* 15:341–361.

Schwieterman, E.W., Robinson, T.D., Meadows, V.S., Misra, A., and Domagal-Goldman, S. (2015b) Detecting and constraining N_2 abundances in planetary atmospheres using collisional pairs. *Astrophys J* 810, doi:10.1088/0004-637X/810/1/57.

Schwieterman, E.W., Meadows, V.S., Domagal-Goldman, S.D., Deming, L.D., Arney, G.N., Luger, R., Harman, C.E., Misra, A., and Barnes, R. (2016a) Identifying planetary biosignature impostors: spectral features of CO and O_4 resulting from abiotic O_2/O_3 production. *Astrophys J* 819:L13.

Schwieterman, E.W., Meadows, V.S., Domagal-Goldman, S.D., Deming, D., Arney, G.N., Luger, R., Harman, C.E., Misra, A., and Barnes, R. (2016b). Erratum: Identifying planetary biosignature impostors: spectral features of CO and O_4

resulting from abiotic O_2/O_3 production (2016, ApJL, 819, L13). *Astrophys J* 821:L34.

Seager, S. (2013) Exoplanet habitability. *Science* 340:577–581.

Seager, S. and Bains, W. (2015) The search for signs of life on exoplanets at the interface of chemistry and planetary science. *Sci Adv* 1, doi:10.1126/sciadv.1500047.

Seager, S., Schrenk, M., and Bains, W. (2012) An astrophysical view of Earth-based metabolic biosignature gases. *Astrobiology* 12:61–82.

Seager, S., Bains, W., and Hu, R. (2013a) A biomass-based model to estimate the plausibility of exoplanet biosignature gases. *Astrophys J* 775, doi:10.1088/0004-637X/775/2/104.

Seager, S., Bains, W., and Hu, R. (2013b) Biosignature gases in H_2-dominated atmospheres on rocky exoplanets. *Astrophys J* 777, doi:10.1088/0004-637X/777/2/95.

Seager, S., Cash, W., Domagal-Goldman, S., Kasdin, N.J., Kuchner, M., Roberge, A., Shaklan, S., Sparks, W., Thomson, M., Turnbull, M., and Warfield, K. (2015) *Exo-S: Starshade Probe-Class Exoplanet Direct Imaging Mission Concept Final Report,* CL #15-1155, Jet Propulsion Laboratory, California Institute of Technology, Pasadena, CA. Available online at exep.jpl.nasa.gov/stdt

Segura, A., Krelove, K., Kasting, J.F., Sommerlatt, D., Meadows, V., Crisp, D., Cohen, M., and Mlawer, E. (2003) Ozone concentrations and ultraviolet fluxes on Earth-like planets around other stars. *Astrobiology* 3:689–708.

Segura, A., Kasting, J.F., Meadows, V., Cohen, M., Scalo, J., Crisp, D., Butler, R.A.H., and Tinetti, G. (2005) Biosignatures from Earth-like planets around M dwarfs. *Astrobiology* 5:706–725.

Segura, A., Meadows, V., Kasting, J., Crisp, D., and Cohen, M. (2007) Abiotic formation of O_2 and O_3 in high-CO_2 terrestrial atmospheres. *Astron Astrophys* 472:665–679.

Selsis, F., Despois, D., and Parisot, J.P. (2002) Signature of life on exoplanets: can Darwin produce false positive detections? *Astron Astrophys* 388:985–1003.

Sheldon, N.D. (2006) Precambrian paleosols and atmospheric CO_2 levels. *Precambrian Res* 147:148–155.

Shields, A.L., Ballard, S., and Johnson, J.A. (2016) The habitability of planets orbiting M-dwarf stars. *Phys Rep* 663:1–38.

Shkolnik, E.L., Rolph, K.A., Peacock, S., and Barman, T.S. (2014) Predicting Lyα and Mg II fluxes from K and M dwarfs using Galaxy Evolution Explorer ultraviolet photometry. *Astrophys J* 796:L20.

Sleep, N.H. (2010) The Hadean-Archaean environment. *Cold Spring Harb Perspect Biol* 2, doi:10.1101/cshperspect.a002527.

Sleep, N.H., Bird, D.K., and Pope, E. (2012) Paleontology of Earth's mantle. *Annu Rev Earth Planet Sci* 40:277–300.

Smith, K.M. and Newnham, D.A. (2000) Near-infrared absorption cross sections and integrated absorption intensities of molecular oxygen (O_2, O_2-O_2, and O_2-N_2). *J Geophys Res: Atmospheres* 105:7383–7396.

Snellen, I. (2014) High-dispersion spectroscopy of extrasolar planets: from CO in hot Jupiters to O_2 in exo-Earths. *Philos Transact A Math Phys Eng Sci* 372, doi:10.1098/rsta.2013.0075.

Snellen, I., de Kok, R., Birkby, J.L., Brandl, B., Brogi, M., Keller, C., Kenworthy, M., Schwarz, H., and Stuik, R. (2015) Combining high-dispersion spectroscopy with high contrast imaging: probing rocky planets around our nearest neighbors. *Astron Astrophys* 576:A59.

Snellen, I.A.G., de Kok, R.J., Le Poole, R., Brogi, M., and Birkby, J. (2013) Finding extraterrestrial life using ground-based high-dispersion spectroscopy. *Astrophys J* 764 doi:10.1088/0004-637X/764/2/182.

Som, S.M., Catling, D.C., Harnmeijer, J.P., Polivka, P.M., and Buick, R. (2012) Air density 2.7 billion years ago limited to less than twice modern levels by fossil raindrop imprints. *Nature* 484:359–362.

Som, S.M., Buick, R., Hagadorn, J.W., Blake, T.S., Perreault, J.M., Harnmeijer, J.P., and Catling, D.C. (2016) Earth's air pressure 2.7 billion years ago constrained to less than half of modern levels. *Nat Geosci* 9:448–451.

Spergel, D., Gehrels, N., Baltay, C., Bennett, D., Breckinridge, J., Donahue, M., Dressler, A., Gaudi, B.S., Greene, T., Guyon, O., and Hirata, C. (2015) Wide-Field InfrarRed survey telescope-astrophysics focused telescope assets WFIRST-AFTA 2015 report. arXiv preprint arXiv:1503.03757.

Stapelfeldt, K., Belikov, R., Bryden, G., Cahoy, K., Chakrabarti, S., Marley, M., McElwain, M., Meadows, V., Serabyn, E., Trauger, J., Brenner, M., Warfield, K., Dekens, F., Brugarolas, P., Dubovitsky, S., Effinger, R., Hirsch, B., Kissel, A., Krist, J., Lang, J., Nissen, J., Oseas, J., Sunada, E., Domagal-Goldman, S., Kuchner, M., Lawson, P., Roberge, A., Sandhu, J., and Seager, S. (2015) *Exo-C: Imagining Nearby Worlds. Exoplanet Direct Imaging: Coronograph Probe Mission Study ''Exo-C,'' Mission Study Final Report, NASA Exoplanet Exploration Program internal document*, CL #14-1550, Jet Propulsion Laboratory, California Institute of Technology, Pasadena, CA. Available online at https://exep.jpl.nasa.gov/stdt/Exo-C_InterimReport.pdf

Stark, C.C., Roberge, A., Mandell, A., and Robinson, T.D. (2014) Maximizing the exoEarth candidate yield from a future direct imaging mission. *Astrophys J* 795, doi:10.1088/0004-637X/795/2/122.

Stark, C.C., Roberge, A., Mandell, A., Clampin, M., Domagal-Goldman, S.D., McElwain, M.W., and Stapelfeldt, K.R. (2015) Lower limits on aperture size for an exoEarth detecting coronagraphic mission. *Astrophys J* 808, doi:10.1088/0004-637X/808/2/149.

Stein, L.Y. and Yung, Y.L. (2003) Production, isotopic composition, and atmospheric fate of biologically produced nitrous oxide. *Annu Rev Earth Planet Sci* 31:329–356.

Stolarski, R.S. and Cicerone, R.J. (1974) Stratospheric chlorine: a possible sink for ozone. *Can J Chem* 52:1610–1615.

Stüeken, E.E., Buick, R., and Anbar, A.D. (2015a) Selenium isotopes support free O_2 in the latest Archean. *Geology* 43:259–262.

Stüeken, E.E., Buick, R., Guy, B.M., and Koehler, M.C. (2015b) Isotopic evidence for biological nitrogen fixation by molybdenum-nitrogenase from 3.2 Gyr. *Nature* 520:666–669.

Thalman, R. and Volkamer, R. (2013) Temperature dependent absorption cross-sections of O_2–O_2 collision pairs between 340 and 630 nm and at atmospherically relevant pressure. *Phys Chem Chem Phys* 15:15371–15381.

Thornton, J.A., Wooldridge, P.J., Cohen, R.C., Martinez, M., Harder, H., Brune, W.H., Williams, E.J., Roberts, J.M., Fehsenfeld, F.C., Hall, S.R., Shetter, R.E., Wert, B.P., and Fried, A. (2002) Ozone production rates as a function of NOx abundances and HOx production rates in the Nashville urban plume. *J Geophys Res: Atmospheres* 107, doi:10.1029/2001JD000932.

Tian, F. (2015) History of water loss and atmospheric O_2 buildup on rocky exoplanets near M dwarfs. *Earth Planet Sci Lett* 432:126–132.

Tian, F., France, K., Linsky, J.L., Mauas, P.J.D., and Vieytes, M.C. (2014) High stellar FUV/NUV ratio and oxygen contents in the atmospheres of potentially habitable planets. *Earth Planet Sci Lett* 385:22–27.

Tinetti, G., Meadows, V.S., Crisp, D., Fong, W., Fishbein, E., Turnbull, M., and Bibring, J.P. (2006a) Detectability of planetary characteristics in disk-averaged spectra. I: The Earth model. *Astrobiology* 6:34–47.

Tinetti, G., Meadows, V.S., Crisp, D., Kiang, N.Y., Kahn, B.H., Bosc, E., Fishbein, E., Velusamy, T., and Turnbull, M. (2006b) Detectability of planetary characteristics in disk-averaged spectra II: synthetic spectra and light-curves of Earth. *Astrobiology* 6:881–900.

Tomkins, A.G., Bowlt, L., Genge, M., Wilson, S.A., Brand, H.E., and Wykes, J.L. (2016) Ancient micrometeorites suggestive of an oxygen-rich Archaean upper atmosphere. *Nature* 533:235–238.

Trauger, J.T. and Lunine, J.I. (1983) Spectroscopy of molecular oxygen in the atmospheres of Venus and Mars. *Icarus* 55:272–281.

Turner, G. (1989) The outgassing history of the Earth's atmosphere. *Journal of the Geological Society* 146:147–154.

Villanueva, G.L., Mumma, M.J., Novak, R.E., Radeva, Y.L., Käufl, H.U., Smette, A., Tokunaga, A., Khayat, A., Encrenaz, T., and Hartogh, P. (2013) A sensitive search for organics (CH_4, CH_3OH, H_2CO, C_2H_6, C_2H_2, C_2H_4), hydroperoxyl (HO_2), nitrogen compounds (N_2O, NH_3, HCN) and chlorine species (HCl, CH_3Cl) on Mars using ground-based high-resolution infrared spectroscopy. *Icarus* 223:11–27.

Vincent, W.F. (2002) Cyanobacterial dominance in the polar regions. In *The Ecology of Cyanobacteria,* edited by M. Potts and B. Whitton, Kluwer Academic Publishers, Dordrecht, the Netherlands, pp 321–340.

Walker, J.C. (1977) *Evolution of the Atmosphere,* Macmillan, New York.

Walkowicz, L.M., Johns-Krull, C.M., and Hawley, S.L. (2008) Characterizing the near-UV environment of M dwarfs. *Astrophys J* 677, doi:10.1086/526421.

Wang, Y., Tian, F., Li, T., and Hu, Y. (2016) On the detection of carbon monoxide as an anti-biosignature in exoplanetary atmospheres. *Icarus* 266:15–23.

Ward, D.M. and Castenholz, R.W. (2000) Cyanobacteria in geothermal habitats. In *The Ecology of Cyanobacteria,* edited by M. Potts and B. Whitton, Kluwer Academic Publishers, Dordrecht, the Netherlands, pp 37–59.

Westall, F., Cavalazzi, B., Lemelle, L., Marrocchi, Y., Rouzaud, J.N., Simionovici, A., Salomé, M., Mostefaoui, S., Andreazza, C., Foucher, F., and Toporski, J. (2011) Implications of *in situ* calcification for photosynthesis in a ~3.3 Ga-old microbial biofilm from the Barberton greenstone belt, South Africa. *Earth Planet Sci Lett* 310:468–479.

Williams, D.M. and Gaidos, E. (2008) Detecting the glint of starlight on the oceans of distant planets. *Icarus* 195:927–937.

Williams, W.E., Gorton, H.L., and Vogelmann, T.C. (2003) Surface gas-exchange processes of snow algae. *Proc Natl Acad Sci USA* 100:562–566.

Wood, B.E., Redfield, S., Linsky, J.L., Müller, H.R., and Zank, G.P. (2005) Stellar Lyα emission lines in the Hubble Space Telescope archive: intrinsic line fluxes and absorption from the heliosphere and astrospheres. *Astrophys J Suppl Ser* 159, doi:10.1086/430523.

Wordsworth, R., and Pierrehumbert, R. (2014) Abiotic oxygen-dominated atmospheres on terrestrial habitable zone planets. *Astrophys J* 785:L20.

Wordsworth, R.D. (2016) Atmospheric nitrogen evolution on Earth and Venus. *Earth Planet Sci Lett* 447:103–111.

Youngblood, A., France, K., Parke Loyd, R.O., Linsky, J.L., Redfield, S., Schneider, P.C., Wood, B.E., Brown, A., Froning, C., Miguel, Y., Rugheimer, S., and Walkowicz, L. (2016) The MUSCLES Treasury Survey. II. Intrinsic Lyα and extreme ultraviolet spectra of K and M dwarfs with exoplanets. *Astrophys J* 824, doi:10.3847/0004-637X/824/2/101.

Yung, Y.L. and DeMore, W.B. (1982) Photochemistry of the stratosphere of Venus: implications for atmospheric evolution. *Icarus* 51:199–247.

Zhu-Barker, X., Cavazos, A.R., Ostrom, N.E., Horwath, W.R., and Glass, J.B. (2015) The importance of abiotic reactions for nitrous oxide production. *Biogeochemistry* 126:251–267.

Zsom, A., Seager, S., De Wit, J., and Stamenković, V. (2013) Toward the minimum inner edge distance of the habitable zone. *Astrophys J* 778, doi:10.1088/0004-637X/778/2/109.

Zugger, M.E., Kasting, J.F., Williams, D.M., Kane, T.J., and Philbrick, C.R. (2011) Searching for water earths in the near-infrared. *Astrophys J* 739, doi:10.1088/0004-637X/739/1/12.

Address correspondence to:
Victoria Meadows
Department of Astronomy and Astrobiology Program
University of Washington
Box 351580
Seattle, WA 98195-1580

E-mail: vsm@astro.washington.edu

Submitted 13 August 2016
Accepted 22 March 2017

Abbreviations Used

FUV = far-UV
HabEx = Habitable Exoplanet Imaging Mission
HDST = High Definition Space Telescope
IWA = inner working angle
JWST = James Webb Space Telescope
LUVOIR = Large Ultraviolet Optical Infrared Survey Telescope
MIR = mid-IR
MUV = mid-UV
NIR = near-IR
NUV = near-UV
PAL = present atmospheric level
WFIRST = Wide Field InfrarRed Survey Telescope